

## Conformal extensions of exact solutions

Exact solutions to the Einstein field equations are the prime source of geometric and physical intuition in general relativity. This chapter revisits some of the classical exact solutions of general relativity (the Minkowski, de Sitter, anti-de Sitter and Schwarzschild spacetimes) from the point of view of conformal geometry. In addition, a general discussion of the construction of Penrose diagrams of static spherically symmetric spacetimes is provided. Most of the material in this chapter can be considered as *classic* – complementary discussions can be found in, for example, Hawking and Ellis (1973) and Griffiths and Podolský (2009). In view of the applications in the later parts of the book, particular emphasis is given to the construction of explicit congruences of conformal geodesics in the exact solutions.

### 6.1 Preliminaries

#### 6.1.1 Spherical symmetry

In what follows, let  $SO(3)$  denote the group of homogeneous linear transformations of  $\mathbb{R}^3$  onto itself which preserve the Euclidean length of vectors and the orientation of the space. A spacetime  $(\mathcal{M}, g)$  is said to be **spherically symmetric** if the group  $SO(3)$  acts by isometry on  $(\mathcal{M}, g)$  with simply connected, complete, spacelike two-dimensional orbits; see, for example, Ehlers (1973). Two points  $p, q \in \mathcal{M}$  are said to be in the same orbit if there is an element of the group  $SO(3)$  taking  $p$  to  $q$ . Given a spherically symmetric spacetime it is natural to introduce the **quotient manifold**  $\mathcal{Q} \equiv \mathcal{M}/SO(3)$ , that is, the manifold obtained from  $\mathcal{M}$  by identifying points on the same orbit. The manifold  $\mathcal{Q}$  inherits from  $(\mathcal{M}, g)$  a two-dimensional Lorentzian metric  $\gamma$ , the **quotient metric**. Let  $\Gamma$  denote the subset of  $\mathcal{Q}$  corresponding to the fixed points of the action of  $SO(3)$ . If  $\Gamma$  is non-empty, then it can be shown that it is a connected timelike boundary of  $\mathcal{Q}$  – the **centre of symmetry**. A spherically symmetric spacetime can have none, one or two centres; see Künzle (1967).

Given a spherically symmetric spacetime  $(\mathcal{M}, g)$ , there exists a function  $\varrho : \mathcal{Q} \rightarrow \mathbb{R}$  such that the spacetime metric  $g$  can be written in the **warped product form**

$$g = \gamma + \varrho^2 \sigma, \tag{6.1}$$

where  $\sigma$  is the **standard metric** of  $\mathbb{S}^2$  given, in the usual spherical coordinates  $(\theta, \varphi)$ , by

$$\sigma = d\theta \otimes d\theta + \sin^2 \theta d\varphi \otimes d\varphi.$$

The function  $\varrho$  is not necessarily an areal coordinate.

### 6.1.2 The 3-sphere

The unit **3-sphere**  $\mathbb{S}^3$  is the three-dimensional submanifold of  $\mathbb{R}^4$  defined by

$$\mathbb{S}^3 \equiv \{(w, x, y, z) \in \mathbb{R}^4 \mid w^2 + x^2 + y^2 + z^2 = 1\}.$$

The **standard Euclidean metric** in  $\mathbb{R}^4$  induces, in a natural way, a 3-metric  $\mathfrak{h}$  on  $\mathbb{S}^3$ , the **standard metric** of  $\mathbb{S}^3$ . The metric  $\mathfrak{h}$  is best expressed using **spherical coordinates**  $(\psi, \theta, \varphi)$  such that

$$w = \cos \psi, \quad x = \sin \psi \cos \theta, \quad y = \sin \psi \sin \theta \cos \varphi, \quad z = \sin \psi \sin \theta \sin \varphi,$$

taking the range  $0 \leq \psi \leq \pi$ ,  $0 \leq \theta \leq \pi$  and  $0 \leq \varphi < 2\pi$ . For simplicity of presentation, in what follows the degeneracy of the spherical coordinate system  $(\psi, \theta, \varphi)$  will be ignored as it can be dealt with by introducing further coordinate charts. In terms of these coordinates one has

$$\mathfrak{h} = d\psi \otimes d\psi + \sin^2 \psi \sigma.$$

Conventionally, the point given by  $\psi = 0$  will be called the **north pole**, while the one with  $\psi = \pi$  will be called the **south pole**.

At every point  $p \in \mathbb{S}^3$  the restriction of the coordinates  $(w, x, y, z)$  can be used to construct suitable **local coordinates**. For example, if  $w(p) > 0$ , then the coordinates  $(x^\alpha) = (x, y, z)$  constitute a well-defined system of local coordinates on the northern hemisphere of  $\mathbb{S}^3$ .

#### A frame on $\mathbb{S}^3$

A direct computation shows that the vector fields on  $T(\mathbb{R}^4)$

$$c_1 \equiv w \frac{\partial}{\partial z} - z \frac{\partial}{\partial w} + x \frac{\partial}{\partial y} - y \frac{\partial}{\partial x}, \tag{6.2a}$$

$$c_2 \equiv w \frac{\partial}{\partial y} - y \frac{\partial}{\partial w} + z \frac{\partial}{\partial x} - x \frac{\partial}{\partial z}, \tag{6.2b}$$

$$c_3 \equiv w \frac{\partial}{\partial x} - x \frac{\partial}{\partial w} + y \frac{\partial}{\partial z} - z \frac{\partial}{\partial y}, \tag{6.2c}$$

are linearly independent and tangent to  $\mathbb{S}^3$ ; hence, they can be regarded as globally defined vectors on  $T(\mathbb{S}^3)$ . This point of view will be used systematically in this book. As  $\mathbf{c}_i \neq 0$  on  $\mathbb{S}^3$  one has, in fact, a globally defined frame on the 3-sphere. Moreover, it can be shown that

$$\mathfrak{h}(\mathbf{c}_i, \mathbf{c}_j) = \delta_{ij}.$$

Accordingly, the vectors  $\{\mathbf{c}_i\}$  are  $\mathfrak{h}$ -orthogonal. A direct calculation shows that

$$[\mathbf{c}_1, \mathbf{c}_2] = 2\mathbf{c}_3, \quad [\mathbf{c}_2, \mathbf{c}_3] = 2\mathbf{c}_1, \quad [\mathbf{c}_3, \mathbf{c}_1] = 2\mathbf{c}_2.$$

The above expressions can be more concisely written as

$$[\mathbf{c}_i, \mathbf{c}_j] = 2\epsilon_{ijk} \mathbf{c}_k,$$

where  $\epsilon_{ijk}$  denotes the components of the volume form in  $\mathbb{R}^3$ . In particular, one has that  $\epsilon_{123} = 1$ . The above commutators can be combined with the Cartan structure equations – see Equations (2.41) and (2.42) – to compute the connection coefficients  $\gamma_i^j{}_k$  with respect to the frame  $\{\mathbf{c}_i\}$ . One obtains the concise expression

$$\gamma_i^j{}_k = -\epsilon_i^j{}_k.$$

#### *The compactification of $\mathbb{R}^3$ into $\mathbb{S}^3$*

An important example of conformal compactification is the so-called **point compactification** of the Euclidean space  $\mathbb{R}^3$  into  $\mathbb{S}^3$ . Let

$$\delta = \mathbf{d}r \otimes \mathbf{d}r + r^2 \mathbf{d}\theta \otimes \mathbf{d}\theta + r^2 \sin^2 \theta \mathbf{d}\varphi \otimes \mathbf{d}\varphi$$

denote the standard (negative definite) three-dimensional Euclidean metric in spherical coordinates with  $0 \leq r < \infty$ ,  $0 \leq \theta \leq \pi$  and  $0 \leq \varphi < 2\pi$ .

An explicit computation shows that the Cotton tensor – see Equation (5.18) – of the metrics  $\delta$  and  $\mathfrak{h}$  vanish so that they must be conformally related; compare Theorem 5.1. In order to make this correspondence explicit, write

$$\mathfrak{h} = \omega^2 \delta \tag{6.3}$$

where  $\omega$  is a conformal factor to be determined. Expressing the radial coordinate as  $r = r(\psi)$ , one finds from Equation (6.3) the conditions

$$\omega^2 r'^2 = 1, \quad r^2 \omega^2 = \sin^2 \psi, \tag{6.4}$$

where  $'$  denotes the derivative with respect to  $\psi$ . A solution to the equations in (6.4) is given by

$$\omega = \frac{2}{\alpha} \sin^2 \frac{\psi}{2}, \quad r(\psi) = \alpha \cot \frac{\psi}{2}, \tag{6.5}$$

where  $\alpha$  is a real constant. Notice that  $r \rightarrow \infty$  as  $\psi \rightarrow 0$ . Thus, the transformation given by (6.5) is a compactification of  $\mathbb{R}^3$  sending the north pole of  $\mathbb{S}^3$  to the

point at infinity in  $\mathbb{R}^3$ , while the south pole of  $\mathbb{S}^3$  is sent to the origin of  $\mathbb{R}^3$ . An alternative solution to equations (6.4), sending the south pole to the point at infinity and the north pole to the origin, is given by

$$\omega = \frac{2}{\alpha} \cos^2 \frac{\psi}{2}, \quad r(\psi) = \alpha \tan \frac{\psi}{2}, \quad (6.6)$$

as can be verified by an explicit computation.

### 6.1.3 The Einstein static universe

The *Einstein static universe* – sometimes also called the *Einstein cosmos* or *Einstein cylinder* – is the spacetime  $(\mathcal{M}_\mathcal{E}, \mathbf{g}_\mathcal{E})$  given by

$$\mathcal{M}_\mathcal{E} \equiv \mathbb{R} \times \mathbb{S}^3, \quad \mathbf{g}_\mathcal{E} \equiv dT \otimes dT - \mathbf{h}. \quad (6.7)$$

It can be readily verified that  $\partial_T$  is a timelike Killing vector of  $\mathbf{g}_\mathcal{E}$  so that the solution is indeed static. Moreover, as  $(\mathbb{S}^3, \boldsymbol{\sigma})$  is a homogeneous and isotropic Riemannian manifold, it follows that  $(\mathcal{M}_\mathcal{E}, \mathbf{g}_\mathcal{E})$  is *spatially homogeneous and isotropic*.

A computation shows that

$$\mathbf{Weyl}[\mathbf{g}_\mathcal{E}] = 0, \quad R[\mathbf{g}_\mathcal{E}] = -6, \quad (6.8a)$$

$$\mathbf{Schouten}[\mathbf{g}_\mathcal{E}] = \frac{1}{2}(dT \otimes dT + \mathbf{h}). \quad (6.8b)$$

Hence, one sees that  $(\mathcal{M}_\mathcal{E}, \mathbf{g}_\mathcal{E})$  is conformally flat. A discussion of the properties of the Einstein static universe as a solution to the Einstein field equations with a perfect fluid matter source can be found in, for example, Griffiths and Podolský (2009) and Hawking and Ellis (1973).

Finally, it is observed that the Einstein static universe is spherically symmetric. Comparing the metric  $\mathbf{g}_\mathcal{E}$  in (6.7) with the warped product metric (6.1) it is natural to set

$$\gamma_\mathcal{E} \equiv dT \otimes dT - d\psi \otimes d\psi, \quad \varrho_\mathcal{E} \equiv \sin \psi,$$

so that  $(T, \psi)$  can be used as coordinates of the quotient manifold  $\mathcal{Q}_\mathcal{E} \equiv (\mathbb{R} \times \mathbb{S}^3)/SO(3) \approx \mathbb{R} \times [0, \pi]$ .

#### *A class of conformal geodesics in the Einstein static universe*

In what follows, consider the congruence of curves on  $(\mathcal{M}_\mathcal{E}, \mathbf{g}_\mathcal{E})$  given by

$$x(\tau) = (\tau, x_\star), \quad \tau \in \mathbb{R}, \quad (6.9)$$

with  $x_\star \in \mathbb{S}^3$  fixed. Varying  $x_\star$  over  $\mathbb{S}^3$  one obtains a non-intersecting timelike congruence covering the whole of  $\mathcal{M}_\mathcal{E}$ . It can be verified that the curves (6.9) are geodesics for  $\mathbf{g}_\mathcal{E}$  with proper time  $\tau$  and tangent vector  $\dot{x} = \partial_T$ .

The curves (6.9) can be recast as conformal geodesics. To see this, one follows the argument of Lemma 5.2 and introduces a parameter  $\bar{\tau}$  such that  $\tau = \tau(\bar{\tau})$  and makes use of the ansatz

$$\bar{\beta} \equiv \alpha(\bar{\tau})\dot{\mathbf{x}}^b = \alpha(\bar{\tau})\mathbf{dT}.$$

Substituting the above expression into the conformal geodesic Equations (5.42a) and (5.42b) and taking into account formula (6.8b) for the Schouten tensor of the Einstein universe one finds the equations

$$\tau'' + \alpha\tau'^2 = 0, \quad \alpha' = \frac{1}{2}\tau'(\alpha^2 + 1),$$

with ' denoting differentiation with respect to  $\bar{\tau}$ . A solution to the above equations is given by

$$\tau = 2\arctan\frac{\bar{\tau}}{2}, \quad \alpha = \frac{\bar{\tau}}{2}. \quad (6.10)$$

Now, one has that  $\langle \bar{\beta}, \mathbf{x}' \rangle = \alpha\tau'$  so that the conformal factor  $\bar{\Theta}$  satisfying the condition  $\bar{\Theta}^2 \mathbf{g}_{\mathcal{E}}(\mathbf{x}', \mathbf{x}') = 1$  obeys the equation  $\bar{\Theta}' = \langle \bar{\beta}, \mathbf{x}' \rangle \bar{\Theta}$  with initial condition  $\bar{\Theta}_* = 1$ . The differential equation for  $\bar{\Theta}$  can be solved to give

$$\bar{\Theta} = 1 + \frac{1}{4}\bar{\tau}^2. \quad (6.11)$$

It can be verified that

$$\bar{\beta} = \frac{1}{2}\bar{\tau}\mathbf{dT} = \bar{\Theta}^{-1}\mathbf{d}\bar{\Theta}.$$

Using the conformal factor  $\bar{\Theta}$  one obtains a conformal representation of the Einstein universe with metric  $\bar{\mathbf{g}}_{\mathcal{E}} \equiv \bar{\Theta}^2 \mathbf{g}_{\mathcal{E}}$  so that

$$\bar{\mathbf{g}}_{\mathcal{E}} = \mathbf{d}\bar{\tau} \otimes \mathbf{d}\bar{\tau} - \left(1 + \frac{1}{4}\bar{\tau}^2\right)^2 \mathbf{h},$$

where the parameter  $\bar{\tau}$  has been introduced as the new time coordinate. This conformal representation of the Einstein cylinder will be known as the *expanding Einstein cylinder*. Notice that  $\mathbf{x}' = \bar{\Theta}^{-1}\dot{\mathbf{x}}$  so that  $\bar{\mathbf{g}}_{\mathcal{E}}(\mathbf{x}', \mathbf{x}') = 1$ . It can be readily verified that the congruence is integrable and that the curves are orthogonal to the surfaces of constant  $\bar{\tau}$ .

## 6.2 The Minkowski spacetime

The Minkowski solution  $(\tilde{\mathcal{M}}, \tilde{\eta})$  is the spacetime given by  $\tilde{\mathcal{M}} = \mathbb{R}^4$  and

$$\tilde{\eta} = \eta_{\mu\nu} \mathbf{d}x^\mu \otimes \mathbf{d}x^\nu, \quad (6.12)$$

where  $(x^\mu) = (t, x, y, z)$  and  $\eta_{\mu\nu} \equiv \text{diag}(1, -1, -1, -1)$ . Alternatively, using spherical coordinates one can write

$$\tilde{\eta} = \mathbf{d}t \otimes \mathbf{d}t - r^2 \mathbf{d}r \otimes \mathbf{d}r - r^2 \boldsymbol{\sigma}. \quad (6.13)$$

Using the expression of the Minkowski metric in Cartesian coordinates one readily sees that  $Riem[\tilde{\eta}] = 0$  so that, in particular,  $Ric[\tilde{\eta}] = 0$ ; that is,  $\tilde{\eta}$  is a solution to the vacuum Einstein field equations with vanishing cosmological constant. Moreover, one has that  $Weyl[\tilde{\eta}] = 0$  so that  $\tilde{\eta}$  is conformally flat and, thus, conformal to the metric of the Einstein cylinder. This relation is analysed in the next section.

### 6.2.1 The compactification into the Einstein cylinder

A standard procedure for the construction of conformal extensions of Lorentzian manifolds is to make use of pairs of so-called *null coordinates*. In the present case a convenient choice is given by

$$u \equiv t - r, \quad v \equiv t + r. \tag{6.14}$$

Conventionally, the coordinate is called a *retarded time*, while  $v$  is an *advanced time*. It can be readily verified that  $\tilde{\eta}^\sharp(\mathbf{d}u, \mathbf{d}u) = \tilde{\eta}^\sharp(\mathbf{d}v, \mathbf{d}v) = 0$ . It follows that

$$\tilde{\eta} = \frac{1}{2}(\mathbf{d}u \otimes \mathbf{d}v + \mathbf{d}v \otimes \mathbf{d}u) - \frac{1}{4}(v - u)^2 \sigma.$$

In order to have  $r \geq 0$  one has the restriction  $u \leq v$ . The present analysis is mainly concerned with the behaviour at infinity; thus, it is natural to introduce a further transformation of coordinates:

$$u \equiv \tan U, \quad v \equiv \tan V, \quad U, V \in (-\frac{1}{2}\pi, \frac{1}{2}\pi), \quad U \leq V.$$

From the relations

$$\mathbf{d}u = \frac{1}{\cos^2 U} \mathbf{d}U = (1 + u^2) \mathbf{d}U, \quad \mathbf{d}v = \frac{1}{\cos^2 V} \mathbf{d}V = (1 + v^2) \mathbf{d}V,$$

and the identity

$$v - u = \tan V - \tan U = \frac{\sin(V - U)}{\cos U \cos V},$$

one obtains

$$\tilde{\eta} = \frac{1}{4 \cos^2 U \cos^2 V} (2(\mathbf{d}U \otimes \mathbf{d}V + \mathbf{d}V \otimes \mathbf{d}U) - \sin^2(U - V) \sigma).$$

This last expression suggests defining the *unphysical metric*  $\eta \equiv \Xi_{\mathcal{M}}^2 \tilde{\eta}$  where

$$\Xi_{\mathcal{M}} \equiv 2 \cos U \cos V, \tag{6.15}$$

so that

$$\eta = 2(\mathbf{d}U \otimes \mathbf{d}V + \mathbf{d}V \otimes \mathbf{d}U) - \sin^2(U - V) \sigma.$$

The conformal factor  $\Xi_{\mathcal{M}}$  vanishes whenever  $U = \pm \frac{1}{2}\pi$  or  $V = \pm \frac{1}{2}\pi$ . In order to investigate the situation in more detail one introduces the final change of coordinates

$$\psi \equiv V - U, \quad T \equiv V + U.$$

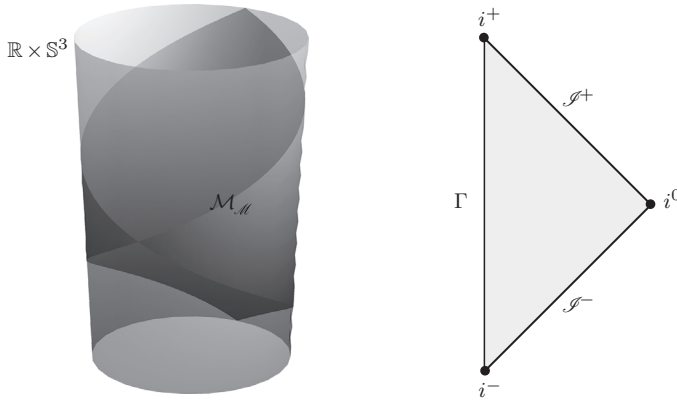


Figure 6.1 Conformal extension of the Minkowski spacetime. Left, conformal embedding of the Minkowski spacetime in the Einstein cylinder: the shaded region corresponds to the set  $\mathcal{M}_{\mathcal{M}}$  of equation (6.21). Right, Penrose diagram of the Minkowski spacetime: the line  $\Gamma$  corresponds to the axis of symmetry, the points  $i^0$ ,  $i^+$  and  $i^-$  are spatial infinity, future timelike infinity and past timelike infinity, respectively. Finally,  $\mathcal{S}^+$  and  $\mathcal{S}^-$  are future and past null infinity; see main text for further details.

Using standard trigonometric identities, one can rewrite the conformal factor (6.15) in terms of the coordinates  $T$  and  $\psi$  to obtain

$$\Xi_{\mathcal{M}} = \cos T + \cos \psi. \tag{6.16}$$

Thus, one ends up with the metric

$$\eta = dT \otimes dT - d\psi \otimes d\psi - \sin^2 \psi \sigma. \tag{6.17}$$

Thus, one has that  $\eta = g_{\mathcal{E}}$ . Consequently, the rescaling procedure described in the previous paragraphs compactifies the Minkowski spacetime into a region of the Einstein cylinder; see Figure 6.1, left panel. The standard coordinates  $(t, r)$  on the Minkowski spacetime are related to the  $(T, \psi)$  coordinates on the Einstein cylinder via the formulae:

$$t = \frac{\sin T}{\cos T + \cos \psi}, \quad r = \frac{\sin \psi}{\cos T + \cos \psi}. \tag{6.18}$$

It follows from the previous discussion that the Minkowski spacetime  $(\mathbb{R}^4, \tilde{\eta})$  is conformal to the domain

$$\tilde{\mathcal{M}}_{\mathcal{M}} \equiv \{p \in \mathcal{M}_{\mathcal{E}} \mid 0 \leq \psi(p) < \pi, \psi(p) - \pi < T(p) < \pi - \psi(p)\},$$

on which  $\Xi_{\mathcal{M}} > 0$ . In addition to  $\tilde{\mathcal{M}}_{\mathcal{M}}$ , it is convenient to single out a number of subsets of  $\mathcal{M}_{\mathcal{E}}$  playing a special role in the discussion of the asymptotic behaviour of the Minkowski spacetime:

(a) **Future and past null infinity** are defined as the hypersurfaces

$$\mathcal{I}^\pm \equiv \{p \in \mathcal{M}_\mathcal{E} \mid 0 < \psi(p) < \pi, T(p) = \pm(\pi - \psi(p))\}, \tag{6.19}$$

on which  $\Xi_{\mathcal{M}} = 0$ . A calculation shows that

$$d\Xi_{\mathcal{M}} = -\sin T dT - \sin \psi d\psi, \tag{6.20}$$

so that  $d\Xi_{\mathcal{M}} \neq 0$  on  $\mathcal{I}^\pm$ . It can, however, be verified that

$$g_\mathcal{E}(d\Xi_{\mathcal{M}}, d\Xi_{\mathcal{M}})|_{\mathcal{I}^\pm} = 0,$$

so that  $\mathcal{I}^\pm$  are null hypersurfaces.

(b) **Spatial infinity** is defined by

$$i^0 \equiv \{p \in \mathcal{M}_\mathcal{E} \mid \psi(p) = \pi, T(p) = 0\}.$$

Inspection of expression (6.7) for the metric  $g_\mathcal{E}$  shows that the radius of the 2-sphere defined by  $T = 0$  and  $\psi = 0$  vanishes. Accordingly,  $i^0$  consists of a single point. Evaluating the differential (6.20) at  $i^0$  one finds that

$$d\Xi_{\mathcal{M}}|_{i^0} = 0, \quad \mathbf{Hess} \Xi_{\mathcal{M}}|_{i^0} = -g_\mathcal{E}|_{i^0}.$$

(c) **Future and past timelike infinity** is defined as

$$i^\pm \equiv \{p \in \mathcal{M}_\mathcal{E} \mid \psi(p) = 0, T(p) = \pm\pi\}.$$

Again, from the metric (6.7) it follows that the 2-spheres defined by  $T = \pm\pi$  and  $\psi = 0$  have vanishing radius so that both  $i^+$  and  $i^-$  correspond to points. Using (6.20) one finds that

$$d\Xi_{\mathcal{M}}|_{i^\pm} = 0, \quad \mathbf{Hess} \Xi_{\mathcal{M}}|_{i^\pm} = g_\mathcal{E}|_{i^\pm}.$$

The motivation for the above definitions follows from the analysis of geodesics; see below. It is important to point out that by convention  $i^0, i^\pm \notin \mathcal{I}^\pm$ . Finally, it is convenient to define the manifold with boundary

$$\mathcal{M}_\mathcal{M} = \tilde{\mathcal{M}}_\mathcal{M} \cup \mathcal{I}^+ \cup \mathcal{I}^- \cup i^+ \cup i^- \cup i^0, \tag{6.21}$$

which will be called the **conformally extended Minkowski manifold**.

*The Penrose diagram of the Minkowski spacetime*

The spherical symmetry of the Minkowski spacetime can be exploited to provide a diagrammatic representation of the global structure of the spacetime known as a **Penrose (or Penrose-Carter) diagram**. It follows from the discussion in Section 6.1.1 that the action of the group  $SO(3)$  on  $\mathcal{M}_\mathcal{M}$  gives rise to the quotient manifold with coordinates  $(T, \psi)$  given by

$$\mathcal{Q}_\mathcal{M} \equiv \{p \in \mathcal{Q}_\mathcal{E} \mid 0 \leq \psi(p) \leq \pi, \psi(p) - \pi \leq T(p) \leq \pi - \psi(p)\}.$$

In what follows, in a slight abuse of notation, the projections of  $\mathcal{I}^\pm, i^\pm, i^0 \subset \mathcal{M}_\mathcal{M}$  on the quotient manifold  $\mathcal{Q}_\mathcal{M}$  will be denoted, again, by the same symbols.

Clearly,  $\mathcal{S}^+$ ,  $i^\pm$ ,  $i^0 \subset \partial\mathcal{Q}_{\mathcal{M}}$ ; however,  $\partial\mathcal{Q}_{\mathcal{M}}$  has a further component consisting of the centre of symmetry

$$\Gamma \equiv \{p \in \mathcal{Q}_{\mathcal{M}} \mid \psi(p) = 0, \quad -\pi < T(p) < \pi\}.$$

As the conformal metric  $\eta$  is the standard one on the Einstein cylinder, it follows from the discussion in Section 6.1.3 that the quotient metric inherited by  $\eta$  on  $\mathcal{Q}_{\mathcal{M}}$  is the two-dimensional Minkowski metric

$$\gamma_{\mathcal{M}} = dT \otimes dT - d\psi \otimes d\psi.$$

Given the above, the Penrose diagram of the Minkowski spacetime is simply the depiction of  $\mathcal{Q}_{\mathcal{M}}$  as a subset of  $\mathbb{R}^2$  as shown in Figure 6.1, right panel. A discussion of the construction of Penrose diagrams for more general spacetimes is given in Section 6.5.2.

#### *Analysis of the behaviour of geodesics*

Intuition on the various features of the construction described in the previous paragraphs can be obtained by analysing the behaviour of various types of physical metric geodesics. To this end one notices the following formulae that can be verified using the coordinate transformations taking the original Minkowski metric of Equation (6.13) into the metric (6.17):

$$\sin T = \frac{2t}{\sqrt{(1+(t-r)^2)(1+(t+r)^2)}}, \quad (6.22a)$$

$$\cos T = \frac{1-t^2+r^2}{\sqrt{(1+(t-r)^2)(1+(t+r)^2)}}, \quad (6.22b)$$

$$\cos \psi = \frac{1+t^2-r^2}{\sqrt{(1+(t-r)^2)(1+(t+r)^2)}}. \quad (6.22c)$$

(a) **Spacelike geodesics.** Radial spacelike geodesics in the Minkowski spacetime can be described using the radial coordinate  $r$  as a parameter. It follows then that the time coordinate of the curves is given by

$$t = ar + t_*, \quad a^2 < 1, \quad t_* \in \mathbb{R}.$$

For  $r \rightarrow \infty$  it follows from (6.22a)–(6.22c) that

$$\sin T \rightarrow 0, \quad \cos T \rightarrow 1, \quad \cos \psi \rightarrow -1.$$

Hence one concludes that  $T \rightarrow 0$  and  $\psi \rightarrow \pi$  as the curve escapes to infinity. Thus, in the unphysical picture, spacelike radial geodesics finish at the same point, spatial infinity  $i^0$ , independently of the value of  $a$ .

- (b) **Timelike geodesics.** For concreteness, consider the family of geodesics described by

$$t = ar + t_*, \quad |a| > 1.$$

It can be verified that as  $r \rightarrow \infty$  one has the limits

$$\sin T \rightarrow 0, \quad \cos T \rightarrow -1, \quad \cos \psi \rightarrow 1.$$

Depending on whether  $\sin T$  approaches 0 from the right or the left, the latter limits correspond to either  $T \rightarrow \pi$  and  $\psi \rightarrow 0$  or  $T \rightarrow -\pi$  and  $\psi \rightarrow 0$ . Thus, the timelike geodesics start and finish, respectively, at  $i^-$  and  $i^+$ .

- (c) **Null geodesics.** Consider, for example, the family of outgoing null geodesics described by the condition  $u = u_*$ , where  $u_*$  is a constant and  $u$  is the null coordinate defined in (6.14). Now, taking the limit  $v \rightarrow \infty$  one finds that

$$\sin T \rightarrow \frac{1}{\sqrt{1 + u_*^2}}, \quad \cos T \rightarrow \frac{u_*}{\sqrt{1 + u_*^2}}, \quad \cos \psi \rightarrow -\frac{u_*}{\sqrt{1 + u_*^2}}.$$

Thus, in the limit one has that  $T = \pi - \psi$ , corresponding to future null infinity  $\mathcal{I}^+$ . Similarly, for incoming geodesics described by the condition  $v = v_*$ ,  $v_*$  a constant and with  $v$  as defined in (6.14), one finds that the limit points lie on the line  $T - \psi = \pi$ , corresponding to past null infinity  $\mathcal{I}^-$ . Summarising, incoming null geodesics start at  $\mathcal{I}^-$  while outgoing null geodesics end at  $\mathcal{I}^+$ .

### 6.2.2 Compactifications adapted to spatial infinity

The discussion of the structure of spatial infinity is better carried out in an alternative conformal representation. Intuitively, the region of spacetime associated with the spatial infinity of the Minkowski spacetime  $(\mathbb{R}^4, \tilde{\eta})$  is contained in the domain  $\tilde{D} \equiv \{p \in \mathbb{R}^4 \mid \eta_{\mu\nu}x^\mu(p)x^\nu(p) < 0\}$ , the **complement of the light cone through the origin**, where  $(x^\mu)$  denote the standard Cartesian coordinates. Now, consider the coordinate inversion defined by

$$y^\mu = -\frac{x^\mu}{X^2}, \quad x^\mu = -\frac{y^\mu}{Y^2},$$

where  $X^2 \equiv \eta_{\mu\nu}x^\mu x^\nu$  and  $Y^2 \equiv \eta_{\mu\nu}y^\mu y^\nu$ . This coordinate transformation maps  $\tilde{D}$  onto itself. Moreover, a computation yields

$$dy^\mu = -\frac{1}{X^2} \left( \delta^\mu_\lambda - \frac{2}{X^2} x^\mu \eta_{\lambda\nu} x^\nu \right) dx^\lambda,$$

so that

$$\eta_{\mu\nu} dy^\mu \otimes dy^\nu = X^{-4} \eta_{\mu\nu} dx^\mu \otimes dx^\nu.$$

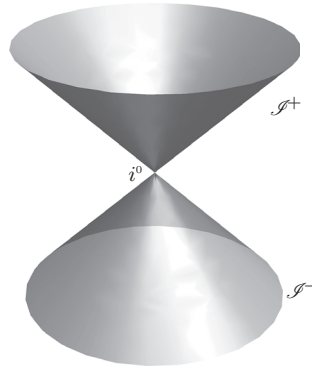


Figure 6.2 The Minkowski spacetime close to null and spatial infinity: the conformal boundary corresponds to the surface of the cones, while the interior of the spacetime corresponds to the exterior of the light cones; see main text for further details.

This computation suggests introducing the conformal factor  $\Xi = 1/X^2$ . Hence, one concludes that

$$\eta = \Xi^2 \tilde{\eta} = \Xi^2 \eta_{\mu\nu} dx^\mu \otimes dx^\nu.$$

Hence, one has a conformal representation of the Minkowski spacetime which is also flat. An inspection shows that the boundary  $\partial\tilde{D}$  decomposes into the sets

$$\begin{aligned} \mathcal{S}^+ &= \{p \in \mathbb{R}^4 \mid y^0(p) > 0, \eta_{\mu\nu} y^\mu(p) y^\nu(p) = 0\}, \\ \mathcal{S}^- &= \{p \in \mathbb{R}^4 \mid y^0(p) < 0, \eta_{\mu\nu} y^\mu(p) y^\nu(p) = 0\}, \\ i^0 &= \{p \in \mathbb{R}^4 \mid (y^\mu(p)) = (0, 0, 0, 0)\}; \end{aligned}$$

see Figure 6.2. An analysis similar to the one carried out in Section 6.2.1 shows that these sets admit the interpretation of future null infinity, past null infinity and spatial infinity, respectively. More precisely,  $\mathcal{S}^+$  ( $\mathcal{S}^-$ ) can be thought of as being generated by the end points of future (past) directed null geodesics while all spatial geodesics eventually run into the point  $i^0$ . The null hypersurfaces  $\mathcal{S}^+$  form the null cone through the point  $i^0$ . Defining the manifold with boundary  $\mathcal{D} \equiv \tilde{D} \cup \partial\tilde{D}$  one observes that the conformal metric  $\eta$  extends smoothly through the boundary.

### 6.2.3 Conformal geodesics in the Minkowski spacetime

Conformal geodesics in the Minkowski spacetime can be computed using the version of the equations adapted to the physical metric; see Section 5.5.6. Using standard Cartesian coordinates so that all the Christoffel symbols vanish, the third-order Equation (5.65) reduces to

$$\tilde{x}''' = \beta^2 \tilde{x}', \quad \beta^2 \equiv -\tilde{\eta}^\sharp(\tilde{\beta}, \tilde{\beta}), \tag{6.23}$$

where it is recalled that  $\beta^2$  is constant along the conformal geodesic and  $'$  denotes differentiation with respect to the physical proper time  $\tilde{\tau}$ . Regarding (6.23) as a second-order equation for  $\tilde{\mathbf{x}}'$  one has that

$$\tilde{\mathbf{x}}' = \mathbf{v}_1 \cosh(\beta\tilde{\tau}) + \mathbf{v}_2 \sinh(\beta\tilde{\tau}),$$

where  $\mathbf{v}_1$  and  $\mathbf{v}_2$  are two constant vectors on the Minkowski spacetime. Making use of the initial conditions  $\tilde{\mathbf{x}}''(0) = \tilde{\boldsymbol{\beta}}_\star^\sharp$  and  $\tilde{\mathbf{x}}'(0) = \mathbf{x}'_\star$  one finds that

$$\tilde{\mathbf{x}}' = \mathbf{x}'_\star \cosh(\beta\tilde{\tau}) + \beta^{-1} \tilde{\boldsymbol{\beta}}_\star^\sharp \sinh(\beta\tilde{\tau}).$$

A final integration taking into account the initial condition  $\tilde{\mathbf{x}}(0) = x_\star$  and Equation (5.63a) yields

$$\begin{aligned} \tilde{\mathbf{x}}(\tilde{\tau}) &= x_\star + \beta^{-1} \mathbf{x}'_\star \sinh(\beta\tilde{\tau}) + \beta^{-2} \tilde{\boldsymbol{\beta}}_\star^\sharp \cosh(\beta\tilde{\tau}) - \beta^2 \tilde{\boldsymbol{\beta}}_\star^\sharp, \\ \tilde{\boldsymbol{\beta}}(\tilde{\tau}) &= \beta \mathbf{x}'_\star \sinh(\beta\tilde{\tau}) + \tilde{\boldsymbol{\beta}}_\star \cosh(\beta\tilde{\tau}), \end{aligned}$$

where in the first expression, in an abuse of notation, the vectors  $\mathbf{x}'_\star$  and  $\tilde{\boldsymbol{\beta}}_\star^\sharp$  are understood as describing points in  $\mathbb{R}^4$ . To rewrite this general solution in terms of the unphysical proper time  $\tau$  one makes use of formula (5.58). A computation yields the formulae:

$$x(\tau) = x_\star + \Theta_\star \Theta^{-1}(\tau) \left( \dot{\mathbf{x}}_\star \tau + \frac{1}{2} \tilde{\boldsymbol{\eta}}(\dot{\mathbf{x}}_\star, \dot{\mathbf{x}}_\star) \boldsymbol{\beta}_\star^\sharp \tau^2 \right), \tag{6.24a}$$

$$\boldsymbol{\beta}(\tau) = (1 + \tau \langle \boldsymbol{\beta}_\star, \dot{\mathbf{x}}_\star \rangle) \boldsymbol{\beta}_\star - \frac{1}{2} \tilde{\boldsymbol{\eta}}^\sharp(\boldsymbol{\beta}_\star, \boldsymbol{\beta}_\star) \dot{\mathbf{x}}_\star \tau, \tag{6.24b}$$

where

$$\Theta(\tau) = \Theta_\star \left( 1 + \langle \boldsymbol{\beta}_\star, \dot{\mathbf{x}}_\star \rangle \tau + \frac{1}{4} \tilde{\boldsymbol{\eta}}(\dot{\mathbf{x}}_\star, \dot{\mathbf{x}}_\star) \tilde{\boldsymbol{\eta}}^\sharp(\boldsymbol{\beta}_\star, \boldsymbol{\beta}_\star) \tau^2 \right).$$

Conformal geodesics which satisfy  $\tilde{\boldsymbol{\eta}}(\dot{\mathbf{x}}, \dot{\mathbf{x}}) = 0$  at some point coincide, following the discussion of Section 5.5.4, with null geodesics. Those with  $\boldsymbol{\beta}_\star = 0$  are standard geodesics of the Minkowski spacetime. Now, if  $\dot{\mathbf{x}}_\star$  is spacelike or timelike one can assume, without loss of generality, that  $\langle \boldsymbol{\beta}_\star, \dot{\mathbf{x}}_\star \rangle = 0$  – following the discussion of Section 5.5.3 this can always be achieved through a reparametrisation of the form given by Equation (5.48) of Lemma 5.1. If  $\dot{\mathbf{x}}_\star$  and  $\boldsymbol{\beta}_\star^\sharp$  generate a timelike 2-surface and  $\dot{\mathbf{x}}_\star$  is timelike, then the conformal geodesic is a hyperbola in the plane tangent to that 2-surface. An example of such type of curve is given by the expression

$$x(\tau) = \left( \frac{4\tau}{4 - a^2\tau^2}, \frac{1}{a} + \frac{2a\tau^2}{4 - a^2\tau^2}, 0, 0 \right), \quad |\tau| \leq \frac{2}{a} \tag{6.25}$$

where  $a^{-2} \equiv -\tilde{\boldsymbol{\eta}}(\dot{\mathbf{x}}, \dot{\mathbf{x}})$ . Examples of these conformal geodesics are depicted in Figure 6.3.

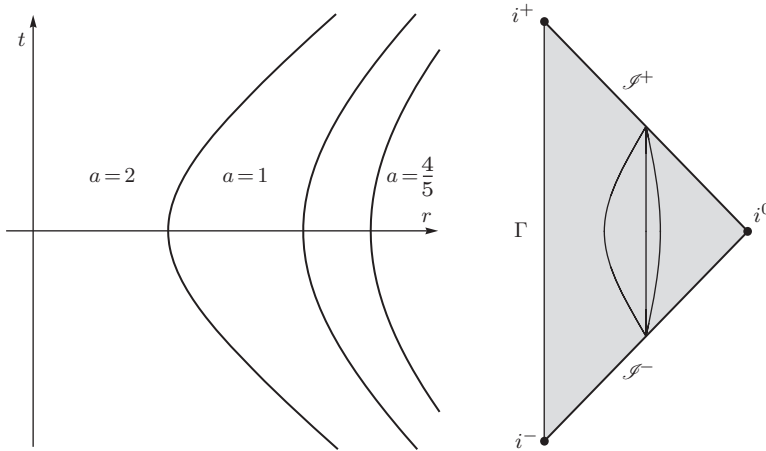


Figure 6.3 Examples of conformal geodesics in the Minkowski spacetime: left, plot in  $(t, r)$ -coordinates of the curve (6.25) for the parameter choices  $a = \frac{4}{5}, 1, 2$ ; right, location of the curves in the Penrose diagram of the Minkowski spacetime. Notice that the curves intersect the conformal boundary at the same points. The diagram is quantitatively correct.

*A special class of conformal geodesics*

As a consequence of the transformation properties of the conformal geodesic equations, the family of curves on the Einstein cylinder given by Equation (6.9) defines a congruence of conformal geodesics on the Minkowski spacetime.

Recalling that  $\bar{g}_\mathcal{E} \equiv \bar{\Theta}^2 g_\mathcal{E}$  and  $g_\mathcal{E} \equiv \Xi_\mathcal{M}^2 \tilde{\eta}$  where  $\bar{\Theta}$  and  $\Xi_\mathcal{M}$  are the conformal factors given, respectively, by Equations (6.11) and (6.16), one has that  $\bar{g}_\mathcal{E} = \Theta_\mathcal{M}^2 \tilde{\eta}$  with  $\Theta_\mathcal{M} \equiv \Xi_\mathcal{M} \bar{\Theta}$ . Along the conformal curves one has that

$$\Xi_\mathcal{M} = \cos \tau + \cos \psi = \left( \frac{4 - \bar{\tau}^2}{4 + \bar{\tau}^2} \right) + \cos \psi,$$

where the second equality is obtained from the reparametrisation formula (6.10) and standard trigonometric identities. Moreover, one finds that along the conformal geodesics

$$\Theta_\mathcal{M} = 2 \cos^2 \frac{\psi}{2} \left( 1 - \frac{1}{4} \tan^2 \frac{\psi}{2} \bar{\tau}^2 \right).$$

To obtain the covector  $\beta_\mathcal{M}$  associated to the solution of the  $\tilde{\eta}$ -conformal geodesic equations let

$$\Upsilon_\mathcal{M} \equiv \Xi_\mathcal{M}^{-1} d\Xi_\mathcal{M} = - \frac{\sin \tau d\tau + \sin \psi d\psi}{\cos \tau + \cos \psi}.$$

Recalling that  $\tau = 2 \arctan \frac{1}{2} \bar{\tau}$  it follows, using standard trigonometric identities, that

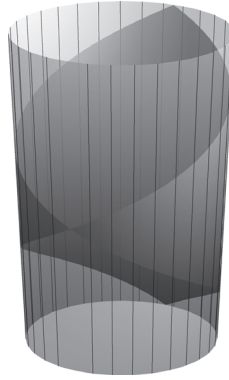


Figure 6.4 A class of conformal geodesics ruling the Einstein cylinder; see main text for further details.

$$\Upsilon_{\mathcal{M}} = -\Theta_{\mathcal{M}}^{-1} \left( \bar{\tau} dT + \left( 1 + \frac{1}{4} \bar{\tau}^2 \right) \sin \psi d\psi \right).$$

Finally, defining  $\beta_{\mathcal{M}} \equiv \bar{\beta} + \Upsilon_{\mathcal{M}}$ , one concludes from the transformation formulae for the solutions of the conformal geodesic equations that the pair  $(x(\bar{\tau}), \beta_{\mathcal{M}}(\bar{\tau}))$  with

$$x(\bar{\tau}) = \left( 2 \arctan \frac{\bar{\tau}}{2}, x_{\star} \right),$$

$$\beta_{\mathcal{M}}(\bar{\tau}) = \left( \arctan \frac{\bar{\tau}}{2} - \Theta_{\mathcal{M}}^{-1} \bar{\tau} \right) dT - \Theta_{\mathcal{M}}^{-1} \left( 1 + \frac{1}{4} \bar{\tau}^2 \right) \sin \psi d\psi,$$

is a solution to the  $\tilde{\eta}$ -conformal geodesic equations. Notice, in particular, that

$$\beta_{\mathcal{M}}(0) = -\frac{\sin \psi}{1 + \cos \psi} d\psi.$$

A depiction of the above class of conformal geodesics is given in Figure 6.4.

### 6.2.4 Hyperboloids in the Minkowski spacetime

An important class of spacelike hypersurfaces in the Minkowski spacetime is given by the *standard hyperboloids*

$$\mathcal{H}_k = \{p \in \mathbb{R}^4 \mid t^2(p) - r^2(p) = k\}, \quad k > 0. \tag{6.26}$$

A direct computation reveals that the unit normal vector to these hypersurfaces is given by

$$\nu^{\#} = \frac{1}{\sqrt{k}} (t \partial_t + r \partial_r).$$

Using this expression one can verify that the extrinsic curvature of the hyperboloids is *pure trace*, that is, proportional to the intrinsic metric of  $\mathcal{H}_k$ . The mean curvature (i.e. the trace of the extrinsic curvature) is given by

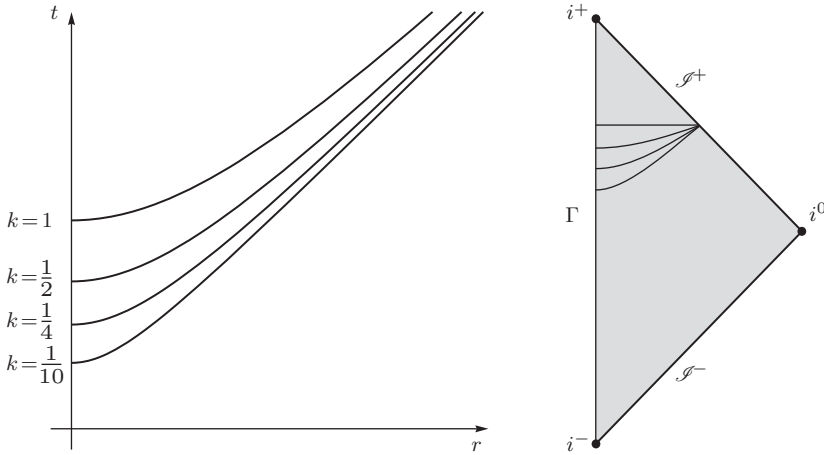


Figure 6.5 Examples of hyperboloids in the Minkowski spacetime: left, the standard hyperboloids  $\mathcal{H}_k$  with  $k = 1, \frac{1}{2}, \frac{1}{4}, \frac{1}{10}$  in  $(t, r)$ -coordinates (see Equation (6.26)); right, location of the hyperboloids in the Penrose diagram. The diagram is quantitatively correct.

$$\tilde{K} = \frac{3}{\sqrt{k}}.$$

That is, the standard hyperboloids are surfaces of *constant mean curvature*. Making use of the coordinates  $(U, V)$  introduced in Section 6.2.1, the defining equation for the hyperboloids can be rewritten as  $\tan U \tan V = k$ . The hyperboloids intersect null infinity whenever  $V = \frac{1}{2}\pi$ . It follows that, in this case,  $U = 0$ . Thus, the hyperboloids  $\mathcal{H}_k$  intersect null infinity at the same points independent of the value of  $k$ . The hypersurfaces differ from each other by the angle  $\alpha$  at which they intersect null infinity. One can compute that

$$\tan \alpha = -\frac{dU}{dV} = k.$$

In particular, if  $k^2 = 1$ , one has that  $\alpha = \frac{1}{4}\pi$ . This particular hyperboloid corresponds to a horizontal line  $T = \frac{1}{2}\pi$  in the Penrose diagram of the Minkowski spacetime; see Figure 6.5.

A more general class of hyperboloids can be obtained by translating the standard hyperboloids (6.26). To this end, one considers the defining equation  $k = (t - t_\star)^2 - r^2$  for fixed  $k$  and  $t_\star$ . Varying  $t_\star$  one obtains a family of **translated hyperboloids**  $\mathcal{H}_{t_\star, k}$ . The intersection of the  $\mathcal{H}_{t_\star, k}$  now depends on the value of  $t_\star$ : if  $V = \frac{1}{2}\pi$ , it follows that  $U = \arctan t_\star$ .

### 6.3 The de Sitter spacetime

The *de Sitter spacetime*  $(\tilde{\mathcal{M}}_{dS}, \tilde{g}_{dS})$  is the solution to the vacuum Einstein field equations  $\mathbf{Ric}[\tilde{g}] = \lambda \tilde{g}$  with negative constant Ricci scalar, in the signature

conventions of this book. The spacetime manifold is given by  $\tilde{\mathcal{M}}_{dS} = \mathbb{R} \times \mathbb{S}^3$  and there exist coordinates where the metric is given by

$$\tilde{g}_{dS} = dt \otimes dt - a^2 \cosh^2(t/a) \mathbf{h}, \quad a \equiv \sqrt{\frac{3}{|\lambda|}}, \quad -\infty < t < \infty, \quad (6.27)$$

with  $\mathbf{h}$  denoting the standard metric of the 3-sphere. Alternatively, there exist further coordinates  $(\bar{t}, \bar{r})$  in terms of which the metric of the de Sitter spacetime takes the form

$$\tilde{g}_{dS} = \left(1 + \frac{1}{3}\lambda\bar{r}^2\right) d\bar{t} \otimes d\bar{t} - \left(1 + \frac{1}{3}\lambda\bar{r}^2\right)^{-1} d\bar{r} \otimes d\bar{r} - \bar{r}^2 \boldsymbol{\sigma}. \quad (6.28)$$

This metric is static for  $\bar{r}^2 > -\frac{1}{3}\lambda$ . A discussion of the relation between various systems of coordinates can be found in Griffiths and Podolský (2009).

To construct a conformal extension of the de Sitter spacetime it is convenient to introduce a new coordinate  $T$  via the condition

$$dt = a \cosh(t/a) dT.$$

Fixing the constant of integration by requiring that  $T = 0$  if  $t = 0$  one obtains

$$T = 2a \arctan e^t - \frac{1}{2}a\pi, \quad t = \ln \tan \left( \frac{T}{2a} + \frac{1}{4}\pi \right),$$

or, equivalently  $\tan(T/2) = \tanh(t/2a)$ . Using standard trigonometric identities the latter can be recast as

$$\cos T = \frac{1}{\cosh(t/a)}.$$

Thus, one concludes that

$$\tilde{g}_{dS} = a^2 \cosh^2 t (dT \otimes dT - \mathbf{h}).$$

The latter expression suggests introducing the conformal factor

$$\Xi_{dS} = \frac{1}{a \cosh(t/a)} = \frac{1}{a} \cos T, \quad (6.29)$$

so that the conformal metric  $\Xi_{dS}^2 \tilde{g}$  is, again, that of the Einstein cylinder. It follows that the locus of points for which  $\Xi_{dS} = 0$  corresponds to  $T = \pm \frac{1}{2}\pi$ ; notice that  $T \rightarrow \pm \frac{1}{2}\pi$  as  $t \rightarrow \pm\infty$ . In view of the latter, one defines **future and past conformal infinity**, respectively, as

$$\mathcal{I}_{dS}^\pm \equiv \left\{ p \in \mathcal{M}_{\mathcal{E}} \mid T(p) = \pm \frac{\pi}{2} \right\}. \quad (6.30)$$

The terminology for these sets will be justified in the next section. From the previous discussion it follows that the de Sitter spacetime is conformal to the domain

$$\tilde{\mathcal{M}}_{dS} \equiv \left\{ p \in \mathcal{M}_{\mathcal{E}} \mid -\frac{\pi}{2} < T(p) < \frac{\pi}{2} \right\}$$

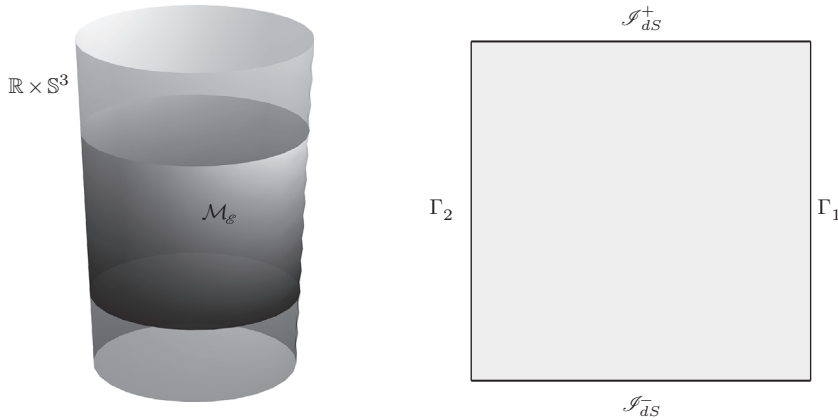


Figure 6.6 Conformal extension of the de Sitter spacetime. Left, conformal embedding of the de Sitter spacetime in the Einstein cylinder: the shaded region corresponds to the set  $\mathcal{M}_{dS}$  of Equation (6.31). Right, Penrose diagram of the de Sitter spacetime: the lines  $\Gamma_1$  and  $\Gamma_2$  correspond to the axes of symmetry, while  $\mathcal{I}_{dS}^+$  and  $\mathcal{I}_{dS}^-$  denote, respectively, future and past conformal infinity; see main text for further details.

of the Einstein cylinder. Moreover, one sets

$$\mathcal{M}_{dS} \equiv \tilde{\mathcal{M}}_{dS} \cup \mathcal{I}_{dS}^+ \cup \mathcal{I}_{dS}^- \tag{6.31}$$

To construct the Penrose diagram of the de Sitter spacetime one considers the quotient domain  $\mathcal{Q}_{dS} \equiv \mathcal{M}_{dS}/SO(3)$ . The boundary  $\partial\mathcal{Q}_{dS}$  of the quotient manifold consists of the projection of the conformal boundary (to be denoted again by  $\mathcal{I}_{dS}^\pm$ ) and the two centres of symmetry  $\Gamma_1$  and  $\Gamma_2$  given, respectively, by the conditions  $\psi = 0$  and  $\psi = \pi$ . A depiction of the Penrose diagram of the de Sitter spacetime is given in Figure 6.6, right panel.

### 6.3.1 Behaviour of geodesics

As in the case of the Minkowski spacetime, intuition about the conformal representation of the de Sitter spacetime can be obtained through the analysis of the behaviour of geodesics. For simplicity set  $\lambda = -3$  so that  $a = 1$  in the line element (6.27). The geodesic equations can be found to be

$$t'^2 - \cosh^2 t \psi'^2 = \epsilon, \quad \psi' = \frac{\ell}{\cosh^2 t},$$

where  $\ell$  is a constant,  $\epsilon$  takes the values 1, 0 or  $-1$  depending on whether one considers timelike, null or spacelike geodesics and  $'$  denotes differentiation with respect to an affine parameter  $s$ . As in the case of the Minkowski spacetime one distinguishes the following three cases:

(a) **Spacelike geodesics.** The geodesic equations can be solved to yield

$$t(s) = \operatorname{arcsinh} \left( \sqrt{\ell^2 - 1} \sin(s - s_*) \right),$$

$$\psi(s) = \psi_* + \arctan(\ell \tan(s - s_*)),$$

with  $s_*$  and  $\psi_*$  real constants. Thus, it follows that the range of the coordinates is bounded and the geodesics remain in a compact region following the same path over and over.

(b) **Timelike geodesics.** For concreteness, consider future-pointing geodesics – the past pointing case is similar. The geodesic equations can be solved to give:

$$t(s) = \operatorname{arcsinh} \left( \sqrt{\ell^2 + 1} \sinh(s - s_*) \right),$$

$$\psi(s) = \psi_* + \arctan(\ell \tanh(s - s_*)).$$

It follows that for  $s \rightarrow \infty$  one has  $t \rightarrow \infty$ . Thus, one obtains the limit points

$$T = \frac{\pi}{2}, \quad \psi = \psi_* + \arctan \ell.$$

The geodesics approach a definite point on the spacelike hypersurface  $\mathcal{S}_{dS}^+$  defined in (6.30).

(c) **Null geodesics.** In this case, the geodesic equations give the solution

$$t(s) = \operatorname{arcsinh} s,$$

$$\psi(s) = \psi_* + \arctan(\ell s).$$

From these expressions it follows, on the one hand, that if  $s \rightarrow \infty$ , then

$$t \rightarrow \infty, \quad T \rightarrow \frac{\pi}{2}, \quad \psi \rightarrow \psi_* + \frac{\pi}{2},$$

while on the other, if  $s \rightarrow -\infty$ , then

$$t \rightarrow -\infty, \quad T \rightarrow -\frac{\pi}{2}, \quad \psi \rightarrow \psi_* - \frac{\pi}{2}.$$

Hence, the null geodesics start and finish, respectively, at  $\mathcal{S}_{dS}^-$  and  $\mathcal{S}_{dS}^+$ , in antipodal points on  $\mathbb{S}^3$ .

### 6.3.2 Conformal geodesics in the de Sitter spacetime

As a consequence of the conformal invariance of conformal geodesics, the curves in the Einstein universe discussed in Section 6.1.3 are also conformal geodesics of the de Sitter spacetime.

Making use of the relations  $\mathbf{g}_{\mathcal{E}} = \Xi_{dS}^2 \tilde{\mathbf{g}}_{dS}$  and  $\bar{\mathbf{g}}_{\mathcal{E}} = \bar{\Theta}^2 \mathbf{g}_{\mathcal{E}}$  where  $\bar{\Theta}$  and  $\Xi_{dS}$  are the conformal factors given, respectively, by Equations (6.11) and (6.29), one

finds that  $\bar{g}_\varepsilon = \Theta_{dS}^2 \tilde{g}_{dS}$  with  $\Theta_{dS} \equiv \bar{\Theta} \Xi_{dS}$ . A calculation using the first of the equations in (6.10) shows that

$$\Xi_{dS} = a \cos \tau = a \left( \frac{4 - \bar{\tau}^2}{4 + \bar{\tau}^2} \right),$$

where in a slight abuse of notation the coordinate  $T$  has been replaced by the parameter of the curves  $\tau$ . Hence, one finds that

$$\Theta_{dS} = a \left( 1 - \frac{1}{4} \bar{\tau}^2 \right),$$

so that  $\Theta_{dS}$  vanishes at  $\bar{\tau} = \pm 2$ . To construct the covector associated to the congruence of conformal geodesics consider  $\Upsilon_{dS} \equiv \Xi_{dS}^{-1} d\Xi_{dS}$ . A calculation then shows that

$$\Upsilon_{dS} = -\frac{16\bar{\tau}}{16 - \bar{\tau}^4} d\bar{\tau} = -\frac{4\bar{\tau}}{4 - \bar{\tau}^2} d\bar{\tau}.$$

Letting  $\beta_{dS} \equiv \bar{\beta} + \Upsilon_{dS}$ , it follows from the transformation laws for conformal geodesics in Section 5.5.2 that the pair  $(x(\bar{\tau}), \beta_{dS}(\bar{\tau}))$ , with

$$x(\bar{\tau}) = \left( 2 \arctan \frac{\bar{\tau}}{2}, x_* \right), \quad \beta_{dS}(\bar{\tau}) = -\left( \frac{2\bar{\tau}}{4 - \bar{\tau}^2} \right) d\bar{\tau}, \quad (6.32)$$

is a solution to the  $\tilde{g}_{dS}$ -conformal geodesic equations with parameter  $\bar{\tau}$ . Notice, in particular, that at the Cauchy surface given by  $\bar{\tau} = 0$  one has that  $\beta_{dS}(0) = 0$ .

Following the discussion from the previous paragraph, the surface given by the condition  $\bar{\tau} = -2$  represents past null infinity  $\mathcal{I}_{dS}^-$ . In some applications, one needs to prescribe initial data for the congruence of conformal geodesics at  $\mathcal{I}_{dS}^-$ . In this case, it is convenient to introduce the further reparametrisation  $\hat{\tau} = \bar{\tau} + 2$  so that

$$\Theta_{dS} = \hat{\tau} - \frac{1}{4} \hat{\tau}^2, \quad \beta_{dS} = -\left( \frac{2\hat{\tau} - 4}{4\hat{\tau} + \hat{\tau}^2} \right) d\hat{\tau}.$$

### 6.4 The anti-de Sitter spacetime

The *anti-de Sitter spacetime* is given by the manifold  $\tilde{\mathcal{M}}_{dS} \approx \mathbb{R}^4$  equipped with the metric

$$\tilde{g}_{dS} = \cosh^2 r dt \otimes dt - a^2 (dr \otimes dr + \sinh^2 r \sigma), \quad a \equiv \sqrt{\frac{3}{\lambda}},$$

with  $t \in \mathbb{R}$  and  $r \in (0, \infty)$ . Strictly speaking, this spacetime is the so-called *universal covering space of the anti-de Sitter spacetime* – the classical anti-de Sitter spacetime has a periodic time coordinate and, thus, closed timelike curves. As in the case of the de Sitter spacetime, it is possible to introduce coordinates  $(\bar{t}, \bar{r})$  in terms of which the metric takes the form

$$\tilde{g}_{dS} = \left( 1 + \frac{1}{3} \lambda \bar{r}^2 \right) d\bar{t} \otimes d\bar{t} - \left( 1 + \frac{1}{3} \lambda \bar{r}^2 \right)^{-1} d\bar{r} \otimes d\bar{r} - \bar{r}^2 \sigma. \quad (6.33)$$

As (in the signature conventions used in this book)  $\lambda > 0$ , there are no horizons in the anti-de Sitter spacetime; see, for example, Griffiths and Podolský (2009).

To obtain a conformal representation of this spacetime, it is convenient to consider a new radial coordinate via the condition

$$dr = \cosh r d\psi,$$

so that  $\psi = 2 \arctan e^r - \frac{1}{2}\pi$ . This condition is equivalent to  $\tan \psi = \sinh r$ . Hence, one has that  $\psi \in [0, \frac{1}{2}\pi]$ . Setting  $T = t/a$ , a calculation then shows that

$$\tilde{g}_{adS} = a^2 \cosh^2 r (dT \otimes dT - \mathbf{h}).$$

The latter suggests introducing the conformal factor

$$\Xi_{adS} = \frac{a}{\cosh r} = a \cos \psi. \quad (6.34)$$

Thus, the conformal metric  $\Xi_{adS}^2 \tilde{g}$  is, again, that of the Einstein cylinder. From the previous discussion it follows that the anti-de Sitter spacetime is conformal to the domain

$$\tilde{\mathcal{M}}_{adS} = \left\{ p \in \mathcal{M}_{\mathcal{E}} \mid 0 \leq \psi(p) < \frac{\pi}{2} \right\},$$

of the Einstein cylinder. Notice, however, that in contrast to the conformal representation of the de Sitter spacetime, the conformal anti-de Sitter spacetime does not cover the whole spatial sections of the cylinder. In particular, one has that the conformal factor  $\Xi_{adS}$  vanishes at  $\psi = \frac{1}{2}\pi$ ; that is, the conformal boundary is, in this case, a timelike hypersurface. Following standard usage, define the *conformal infinity of the anti-de Sitter spacetime* as

$$\mathcal{I}_{adS} \equiv \left\{ p \in \mathcal{M}_{\mathcal{E}} \mid \psi(p) = \frac{\pi}{2} \right\}.$$

One also defines

$$\mathcal{M}_{adS} \equiv \tilde{\mathcal{M}}_{adS} \cup \mathcal{I}_{adS}. \quad (6.35)$$

The Penrose diagram for the anti-de Sitter spacetime is constructed by considering the quotient domain  $\mathcal{Q}_{adS} \equiv \mathcal{M}_{adS}/SO(3)$  with boundary  $\partial\mathcal{Q}_{adS} = \mathcal{I}_{adS} \cup \Gamma$  where  $\mathcal{I}_{adS}$  denotes the projection of null infinity onto  $\mathcal{Q}_{\mathcal{E}}$  and  $\Gamma$  denotes the centre of symmetry given by the condition  $\psi = 0$ . A depiction of the Penrose diagram is given in Figure 6.7.

#### 6.4.1 Geodesics in the anti-de Sitter spacetime

In what follows, for simplicity assume that  $\lambda = 3$  so that  $a = 1$ . Radial geodesics in the anti-de Sitter spacetime are described by the equations

$$\cosh^2 r T'^2 - r'^2 = \epsilon, \quad T' = \frac{\ell}{\cosh^2 r}.$$

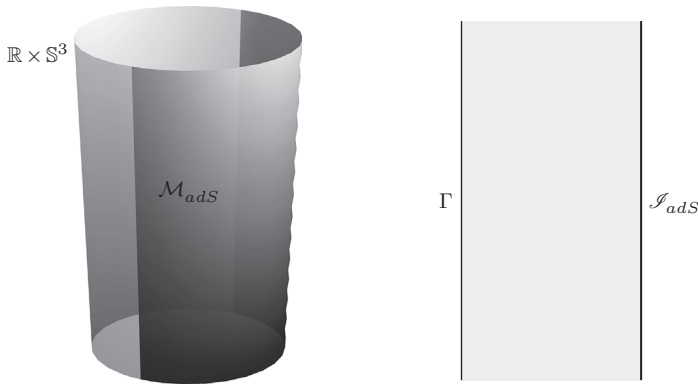


Figure 6.7 Conformal extension of the anti-de Sitter spacetime. Left, conformal embedding of the anti-de Sitter spacetime in the Einstein cylinder: the shaded region corresponds to the set  $\mathcal{M}_{adS}$  of Equation (6.35). Right, Penrose diagram of the anti-de Sitter spacetime: the line  $\Gamma$  corresponds to the axis of symmetry, while  $\mathcal{I}_{adS}$  denotes conformal infinity; see main text for further details.

These equations can be obtained from those of the de Sitter spacetime by the replacements  $t \mapsto r$ ,  $\psi \mapsto T$  and  $\epsilon \mapsto -\epsilon$ ; see Section 6.3.1. Again, one has three cases to consider:

- (a) **Spacelike geodesics.** In this case, the geodesic equations can be solved to give

$$r(s) = \operatorname{arcsinh} \left( \sqrt{\ell^2 + 1} \sinh(s - s_\star) \right),$$

$$T(s) = T_\star + \arctan(\ell \tanh(s - s_\star)),$$

with  $s_\star$  and  $T_\star$  real constants. Thus, for  $s \rightarrow \infty$  one obtains the limits

$$r \rightarrow \infty, \quad \psi \rightarrow \frac{\pi}{2}, \quad T \rightarrow T_\star + \arctan \ell.$$

As a consequence, in the conformal representation, radial spacelike geodesics approach the conformal boundary  $\mathcal{I}_{adS}$ .

- (b) **Timelike geodesics.** For simplicity only future-oriented geodesics are considered. The solution to the geodesic equations is then given by

$$r(s) = \operatorname{arcsinh} \left( \sqrt{\ell^2 - 1} \sin(s - s_\star) \right),$$

$$T(s) = T_\star + \arctan(\ell \tan(s - s_\star)).$$

Accordingly, the coordinate  $r$  is periodic while  $\tau$  grows unbounded – the limit points of these curves are not in the Einstein cylinder.

- (c) **Null geodesics.** In this case, the solution to the geodesic equations is

$$r(s) = \operatorname{arcsinh} s,$$

$$T(s) = T_\star + \arctan s.$$

As a consequence of these equations one has the limits

$$r \rightarrow \infty, \quad \psi \rightarrow \frac{\pi}{2}, \quad T \rightarrow T_* + \frac{\pi}{2},$$

as  $s \rightarrow \infty$ . Thus, in the conformal representation, the null geodesics end at the conformal boundary  $\mathcal{I}_{adS}$ .

#### 6.4.2 Conformal geodesics in the anti-de Sitter spacetime

The methods used to construct conformal geodesics in the Minkowski and the de Sitter spacetimes can also be used in the anti-de Sitter spacetime. For conciseness, the discussion is restricted to the class of conformal geodesics arising from the curves (6.9) in the Einstein universe.

Using that  $\mathbf{g}_\varepsilon = \Xi_{adS}^2 \tilde{\mathbf{g}}_{adS}$  and that  $\bar{\mathbf{g}}_\varepsilon = \bar{\Theta}^2 \mathbf{g}_\varepsilon$  where  $\bar{\Theta}$  and  $\Xi_{adS}$  are the conformal factors given by Equations (6.11) and (6.34), one finds that  $\bar{\mathbf{g}}_\varepsilon = \Theta_{adS}^2 \tilde{\mathbf{g}}_{adS}$ , where

$$\Theta_{adS} \equiv \bar{\Theta} \Xi_{adS} = a \cos \psi \left( 1 + \frac{1}{4} \bar{\tau}^2 \right).$$

Letting

$$\Upsilon_{adS} \equiv \Xi_{adS}^{-1} \mathbf{d}\Xi_{adS} = -\tan \psi \mathbf{d}\psi,$$

one finds that the associated covector is given by

$$\begin{aligned} \beta_{adS} &\equiv \bar{\beta} + \Upsilon_{adS} = \frac{1}{2} \bar{\tau} \mathbf{d}T - \tan \psi \mathbf{d}\psi \\ &= \frac{2\bar{\tau}}{4 + \bar{\tau}^2} \mathbf{d}\bar{\tau} - \tan \psi \mathbf{d}\psi. \end{aligned}$$

The expression for the actual curve is, as in the case of the de Sitter spacetime, given by

$$x(\bar{\tau}) = \left( 2\arctan \frac{\bar{\tau}}{2}, x_* \right). \quad (6.36)$$

An important property of this non-intersecting congruence of conformal geodesics is that *curves that for some value of the parameter  $\bar{\tau}$  are at the conformal boundary  $\mathcal{I}_{adS}$  remain in it for all values of  $\bar{\tau}$ ; this observation follows from the fact that the curve given by Equation (6.36) is constant in the spatial directions.*

**Remark.** As  $\arctan \frac{1}{2} \bar{\tau} \rightarrow \frac{1}{2} \pi$  as  $\bar{\tau} \rightarrow \infty$  and  $\tau = 2\arctan \frac{1}{2} \bar{\tau}$ , the parameter  $\bar{\tau}$  does not cover the whole Einstein cylinder and only exhausts the slab  $[-\pi, \pi] \times \mathbb{S}^3$ . In order to continue the conformal geodesic to other portions of the anti-de Sitter spacetime one has to introduce a reparametrisation of the curve by means of a fractional transformation as discussed in Lemma 5.1.

## 6.5 Conformal extensions of static and stationary black hole spacetimes

A natural extension of the discussion of the previous sections is the analysis of the conformal structure of spacetimes describing black holes. The more complicated topology of these spacetimes and the presence of singularities and horizons make this analysis a much more challenging endeavour. In fact, several aspects of the conformal structure of static and stationary black holes are open research questions.

### 6.5.1 The Schwarzschild spacetime

The Schwarzschild spacetime, being static and spherically symmetric, is the simplest type of black hole spacetime. The *Birkhoff theorem* states that any spherically symmetric solution to the vacuum Einstein field equations with vanishing cosmological constant is, in fact, isometric to the Schwarzschild spacetime; see, for example, Misner et al. (1973). Moreover, the black hole uniqueness theorems show that the Schwarzschild spacetime is the only static black hole spacetime; see, for example, Chruściel et al. (2012b) for an entry point to the extensive literature on this topic.

The *Schwarzschild metric* is given in standard  $(t, r)$  coordinates by the line element

$$\tilde{g}_{\mathcal{S}} = \left(1 - \frac{2m}{r}\right) dt \otimes dt - \left(1 - \frac{2m}{r}\right)^{-1} dr \otimes dr - r^2 \sigma, \quad (6.37)$$

with  $m$  the so-called *mass parameter*. The reader interested in a discussion of the various aspects of the Schwarzschild spacetime is referred to, for example, Griffiths and Podolský (2009) and Hawking and Ellis (1973).

To obtain a conformal extension of the Schwarzschild spacetime it is convenient to make use of coordinates adapted to the light-cone structure of the spacetime. Accordingly, one introduces the *advanced* and *retarded null Eddington-Finkelstein coordinates*

$$u \equiv t - r - 2m \log |r - 2m|, \quad v \equiv t + r + 2m \log |r - 2m|,$$

so that the line element (6.37) transforms into

$$\tilde{g}_{\mathcal{S}} = \frac{1}{2} \left(1 - \frac{2m}{r}\right) (du \otimes dv + dv \otimes du) - r^2 \sigma,$$

where the relation between  $r$  and the coordinates  $(u, v)$  is given implicitly by the condition

$$r + 2m \log |r - 2m| = \frac{1}{2}(v - u).$$

The singular behaviour of the metric at  $r = 2m$  is then removed by means of a reparametrisation of the null coordinates. Namely, one sets

$$U \equiv -4me^{-u/4m}, \quad V \equiv 4me^{v/4m},$$

so that one obtains

$$\tilde{g}_{\mathcal{S}} = \frac{m}{r} e^{-r/2m} (\mathbf{d}U \otimes \mathbf{d}V + \mathbf{d}V \otimes \mathbf{d}U) - r^2 \boldsymbol{\sigma}, \tag{6.38}$$

where  $r$  is now given implicitly by the condition

$$UV = -8m(r - 2m)e^{r/2m}.$$

The horizon is then given by the condition  $UV = 0$  while the singularity corresponds to  $UV = 16m^2$ . The line element in Equation (6.38) is the so-called **Kruskal-Székereš form** of the Schwarzschild spacetime. It provides the maximal analytic extension of the Schwarzschild metric (6.37). Inspection of the admissible range of coordinates in Equation (6.38) shows that the resulting maximal manifold has the topology of  $\mathbb{R} \times \mathbb{R} \times \mathbb{S}^2$ .

To compactify the Kruskal-Székereš form of the Schwarzschild metric one introduces a further coordinate transformation:

$$\bar{U} \equiv \arctan\left(\frac{U}{4m}\right), \quad \bar{V} \equiv \arctan\left(\frac{V}{4m}\right)$$

where

$$-\frac{1}{2}\pi < \bar{U} < \frac{1}{2}\pi, \quad -\frac{1}{2}\pi < \bar{V} < \frac{1}{2}\pi, \quad -\frac{1}{2}\pi < \bar{U} + \bar{V} < \frac{1}{2}\pi.$$

It follows then that

$$\mathbf{d}U = 4m \sec^2 \bar{U} \mathbf{d}\bar{U}, \quad \mathbf{d}V = 4m \sec^2 \bar{V} \mathbf{d}\bar{V},$$

so that the line element (6.38) transforms into

$$\tilde{g}_{\mathcal{S}} = \sec^2 \bar{U} \sec^2 \bar{V} \left( \frac{16m^3}{r} e^{-r/2m} (\mathbf{d}\bar{U} \otimes \mathbf{d}\bar{V} + \mathbf{d}\bar{V} \otimes \mathbf{d}\bar{U}) - r^2 \cos^2 \bar{U} \cos^2 \bar{V} \boldsymbol{\sigma} \right).$$

It is, therefore, natural to consider a conformal factor of the form

$$\Xi_{\mathcal{S}} = \cos \bar{U} \cos \bar{V},$$

so that  $\mathbf{g}_{\mathcal{S}} = \Xi_{\mathcal{S}}^2 \tilde{g}_{\mathcal{S}}$  is given by

$$\mathbf{g}_{\mathcal{S}} = \frac{16m^3}{r} e^{-r/2m} (\mathbf{d}\bar{U} \otimes \mathbf{d}\bar{V} + \mathbf{d}\bar{V} \otimes \mathbf{d}\bar{U}) - r^2 \cos^2 \bar{U} \cos^2 \bar{V} \boldsymbol{\sigma},$$

where  $r = r(\bar{U}, \bar{V})$ . This conformal metric is singular at  $r = 0$  (the singularity). In order to discuss the structure of the conformal boundary of the Schwarzschild spacetime, it is convenient to introduce the coordinates

$$T \equiv \bar{V} + \bar{U}, \quad \psi \equiv \bar{V} - \bar{U},$$

so that  $T \in [-\pi, \pi]$ ,  $\psi \in [-\pi, \pi]$ . One sees that the maximal analytic extension of the Schwarzschild spacetime is conformal to the interior of the domain  $\mathcal{M}_{\mathcal{S}} \subset (-\pi, \pi) \times [-\pi, \pi] \times \mathbb{S}^2$  with boundary given by

$$\partial\mathcal{M}_{\mathcal{S}} = \mathcal{I}_1^+ \cup \mathcal{I}_2^+ \cup \mathcal{I}_1^- \cup \mathcal{I}_2^- \cup i_1^0 \cup i_2^0 \cup i_1^+ \cup i_2^+ \cup i_1^- \cup i_2^-,$$

where by analogy with the analysis of the conformal boundary of the Minkowski spacetime one defines the various components of **null infinity** as

$$\begin{aligned} \mathcal{I}_1^+ &\equiv \left\{ \bar{V} = \frac{1}{2}\pi \right\}, & \mathcal{I}_2^+ &\equiv \left\{ \bar{U} = \frac{1}{2}\pi \right\}, \\ \mathcal{I}_1^- &\equiv \left\{ \bar{U} = -\frac{1}{2}\pi \right\}, & \mathcal{I}_2^- &\equiv \left\{ \bar{V} = -\frac{1}{2}\pi \right\}, \end{aligned}$$

and the two components of **spatial infinity** as

$$i_1^0 \equiv \{T = 0, \psi = \pi\}, \quad i_2^0 \equiv \{T = 0, \psi = -\pi\}.$$

Finally, the **timelike infinities** are given by

$$i_1^\pm \equiv \left\{ T = \pm\pi, \psi = \frac{1}{2}\pi \right\}, \quad i_2^\pm \equiv \left\{ T = \pm\pi, \psi = -\frac{1}{2}\pi \right\}.$$

An analysis of the geodesics on the Schwarzschild spacetime justifies the name given to the various components of  $\partial\mathcal{M}_{\mathcal{S}}$ . Observe that the singularities at  $r = 0$  are not included as part of the boundary  $\partial\mathcal{M}_{\mathcal{S}}$ . In this representation, the spatial infinities  $i_1^0$  and  $i_2^0$  can be seen to correspond to two points on the conformal manifold. Further properties of the conformal structure of the Schwarzschild spacetime – in particular, the nature of  $i^0$  – will be analysed in the context of the *conformal Einstein field equations* in Chapter 20. Finally, the Penrose diagram of the Schwarzschild spacetime can be readily obtained by considering the quotient manifold  $\mathcal{Q}_{\mathcal{S}} = \mathcal{M}_{\mathcal{S}}/SO(3)$ ; the resulting diagram is given in Figure 6.8.

### Conformal geodesics in the Schwarzschild spacetime

A detailed analysis of a class of conformal geodesics in this spacetime can be found in Friedrich (2003a) where it is shown that the Schwarzschild spacetime can be completely covered by a (non-singular) congruence of conformal geodesics. This congruence is adapted to the spherical symmetry of the spacetime.

#### 6.5.2 Conformal extensions of other static, spherically symmetric spacetimes

The procedure to construct a conformal extension of the Schwarzschild spacetime discussed in Section 6.5.1 can be generalised to include a wide class of *static, spherically symmetric* spacetimes. In this section, an adaptation of a general procedure given on Walker (1970) is discussed. This discussion illuminates the conformal diagram of a number of spacetimes.

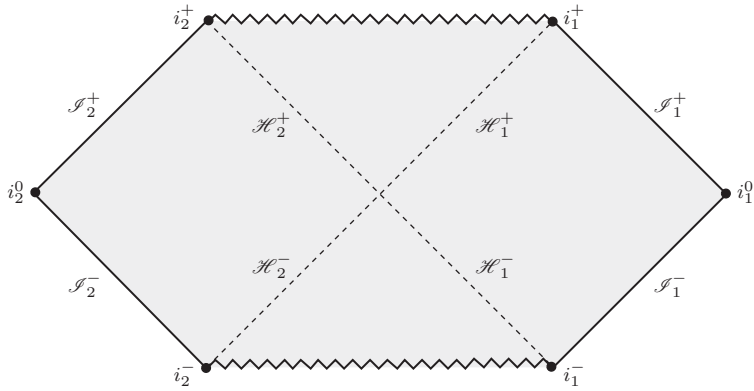


Figure 6.8 Penrose diagram of the Schwarzschild spacetime. The null hyper-surfaces  $\mathcal{S}_1^\pm$  and  $\mathcal{S}_2^\pm$  correspond to the four different components of null infinity, while the points  $i_1^0, i_2^0$  and  $i_1^\pm, i_2^\pm$  denote, respectively, the various locations of spatial and timelike infinities. The serrated lines denote the singularities, and  $\mathcal{H}_1^\pm$  and  $\mathcal{H}_2^\pm$  correspond to the various components of the horizon; see the main text for further details.

In what follows, let  $(\tilde{\mathcal{M}}, \tilde{\mathbf{g}})$  denote a spherically symmetric spacetime endowed with a further Killing vector  $\partial_t$ . The following considerations will be independent of the matter content of the spacetime; hence, the spacetime is not assumed to be a vacuum. Attention will be restricted to spacetimes in which it is possible to find coordinates  $(t, r)$  such that the metric  $\tilde{\mathbf{g}}$  takes the form

$$\tilde{\mathbf{g}} = F(r)\mathbf{dt} \otimes \mathbf{dt} - F(r)^{-1}\mathbf{dr} \otimes \mathbf{dr} - r^2\boldsymbol{\sigma}.$$

The coordinate  $r$  is an areal coordinate; that is, the area of a 2-sphere described by the conditions  $t = \text{constant}, r = \text{constant}$  is  $4\pi r^2$ . The function  $F(r)$  is the norm of the Killing vector  $\partial_t$ . When  $F(r) > 0$  the Killing vector  $\partial_t$  is timelike, and, thus, the metric  $\tilde{\mathbf{g}}$  is *static*.

To simplify the presentation, the subsequent analysis will make use of the quotient manifold  $\tilde{\mathcal{Q}} = \tilde{\mathcal{M}}/SO(3)$ . The two-dimensional quotient metric  $\tilde{\gamma}$  induced by  $\tilde{\mathbf{g}}$  on  $\tilde{\mathcal{Q}}$  is given by

$$\tilde{\gamma} = F(r)\mathbf{dt} \otimes \mathbf{dt} - F(r)^{-1}\mathbf{dr} \otimes \mathbf{dr}.$$

The Levi-Civita connection associated to the Lorentzian metric  $\tilde{\gamma}$  will be denoted by  $\tilde{\mathcal{D}}$ . Let  $\dot{\mathbf{x}} = (\dot{t}, \dot{r})$  denote the tangent vector to an affinely parametrised geodesic in  $\tilde{\mathcal{Q}}$ ; here, and in what follows, a dot ( $\dot{\phantom{x}}$ ) denotes differentiation with respect to an affine parameter. The geodesic equation  $\tilde{\mathcal{D}}_{\dot{\mathbf{x}}}\dot{\mathbf{x}} = 0$  can be integrated once to yield

$$\dot{t} = \varkappa F, \quad \dot{r} = \sqrt{\varkappa^2 - \epsilon F},$$

where  $\varkappa$  is a constant and  $\epsilon \equiv \tilde{\gamma}(\dot{\mathbf{x}}, \dot{\mathbf{x}})$ . As  $\tilde{\gamma}$  is a two-dimensional metric, the only invariant of the curvature of  $\tilde{\gamma}$  is the Ricci scalar  $R[\tilde{\gamma}] = F''$ , where  $'$  denotes

differentiation with respect to  $r$ . In the remainder of this section it will be shown that if  $F$  and  $F''$  are finite for all  $r \in \mathbb{R}$ , then every geodesic in  $\tilde{\mathcal{Q}}$  can be extended until it is complete. If, on the other hand,  $F$  or  $F''$  become unbounded for some value  $r_{\frac{1}{2}}$ , then only those geodesics along which  $r = r_{\frac{1}{2}}$  within a finite affine distance from some point in  $\tilde{\mathcal{Q}}$  are incomplete and inextendible; hence,  $\tilde{\mathcal{Q}}$  and also  $\tilde{\mathcal{M}}$  are singular. The extensions obtained from the following considerations are *maximal*.

**Elementary blocks.** In what follows, assume that  $F$  has a finite number of zeros, to be denoted by  $a_i$ ,  $i = 1, \dots, n$  with  $a_1 < \dots < a_n$ . If  $F$  approaches a constant finite value as  $r \rightarrow \infty$ , so that  $R[\tilde{\gamma}] = F'' \rightarrow 0$ , then one can redefine coordinates so that  $\lim_{r \rightarrow \infty} F = \pm 1$ . In this case  $\tilde{\mathcal{Q}}$  is *asymptotically flat* and a null conformal boundary similar to that of the Minkowski spacetime can be constructed; an analogous discussion can be made in the case  $r \rightarrow -\infty$ . A different possible asymptotic behaviour occurs when  $F$  becomes unbounded as  $r \rightarrow \infty$ . Using the de Sitter and the anti-de Sitter metrics in static form as given by Equations (6.28) and (6.33) one sees that the behaviour  $F \rightarrow -\infty$  and  $F \rightarrow \infty$  as  $r \rightarrow \infty$  corresponds, respectively, to *de Sitter-like* and *anti-de Sitter-like* asymptotic regions. These regions can be compactified to obtain conformal boundaries similar to those of the de Sitter and anti-de Sitter spacetimes, that is, given, respectively, by spacelike and timelike hypersurfaces.

When  $F$  vanishes, the orbits of the timelike Killing vector become null; that is, one has a **Killing horizon**. This suggests dividing  $\tilde{\mathcal{Q}}$  into  $n + 1$  regions (**blocks**). Each of these regions is bounded by two of the Killing horizons, by a Killing horizon and conformal infinity, or by a Killing horizon and a singular line at  $r = r_{\frac{1}{2}}$  for  $r_{\frac{1}{2}}$  fixed. The maximal extension of  $\tilde{\mathcal{Q}}$  is found by *gluing* together elementary blocks along their boundaries (**seams**). In what follows, for a **non-singular seam** it will be understood one where  $F = 0$  and  $F''$  is finite, while a **singular seam** will be one where  $F$  or  $F''$  (or both) are unbounded. Blocks can be glued together only along non-singular seams across which  $F''$  is *smooth*.

In each region

$$\tilde{\mathcal{Q}}_i \equiv \{(t, r) \in \tilde{\mathcal{Q}} \mid t \in \mathbb{R}, r \in [a_i, a_{i+1}]\},$$

fix some value  $r_i \in (a_i, a_{i+1})$  of  $r$  and define *null coordinates* via

$$u_i \equiv t - \int_{r_i}^r F^{-1}(s) ds, \quad v_i \equiv t + \int_{r_i}^r F^{-1}(s) ds.$$

In terms of these new coordinates the metric  $\tilde{\gamma}$  takes the form

$$\tilde{\gamma} = \frac{1}{2} F(r) (\mathbf{d}u_i \otimes \mathbf{d}v_i + \mathbf{d}v_i \otimes \mathbf{d}u_i).$$

This form of the metric is smooth for  $u_i, v_i \in \mathbb{R}$  if  $F(r)$  is smooth. The coordinate  $r$  will be regarded as a function of  $(u_i, v_i)$  given, implicitly, as the solution to the equations

$$\frac{1}{2}(v_i - u_i) = \int_{r_i}^r F^{-1}(s)ds, \quad \frac{1}{2}(u_i + v_i) = t. \tag{6.39}$$

The construction can be extended to singular blocks by setting  $r_i = r_{\frac{1}{2}}$ .

In the non-singular case, the integrals

$$\int_{a_i}^r F^{-1}(s)ds, \quad \int_{r_i}^{a_{i+1}} F^{-1}(s)ds,$$

are divergent as the points  $r = a_i, a_{i+1}$  are poles of the integrand. From this observation together with the formulae in (6.39), assuming  $F > 0$  in  $\tilde{Q}_i$ , one deduces the limits:

- (a) If  $r \rightarrow a_{i+1}$  and  $v_i$  is finite, then  $u_i \rightarrow -\infty$  and  $t \rightarrow -\infty$ .
- (b) If  $r \rightarrow a_{i+1}$  and  $u_i$  is finite, then  $v_i \rightarrow +\infty$  and  $t \rightarrow +\infty$ .
- (c) If  $r \rightarrow a_i$  and  $v_i$  is finite, then  $u_i \rightarrow +\infty$  and  $t \rightarrow +\infty$ .
- (d) If  $r \rightarrow a_i$  and  $u_i$  is finite, then  $v_i \rightarrow -\infty$  and  $t \rightarrow -\infty$ .

The setting described by the above limits is depicted in Figure 6.9, left panel. The coordinates  $(u_i, v_i)$  can be compactified via

$$U_i \equiv \arctan u_i, \quad V_i \equiv \arctan v_i,$$

with  $U_i, V_i \in [-\frac{1}{2}\pi, \frac{1}{2}\pi]$  so that  $\tilde{\gamma}$  can be rewritten as

$$\tilde{\gamma} = \frac{1}{2}F(r) \sec^2 U_i \sec^2 V_i (dU_i \otimes dV_i + dV_i \otimes dU_i). \tag{6.40}$$

In what follows, for simplicity, given a regular block  $\tilde{Q}_i$  with coordinate  $r \in [a_i, a_{i+1}]$ , it is assumed that the zeros of  $F(r)$  are such that

$$F(r) \sec^2 U_i \sec^2 V_i < \infty \quad \text{as} \quad U_i \rightarrow \pm \frac{1}{2}\pi \quad \text{or} \quad V_i \rightarrow \pm \frac{1}{2}\pi.$$

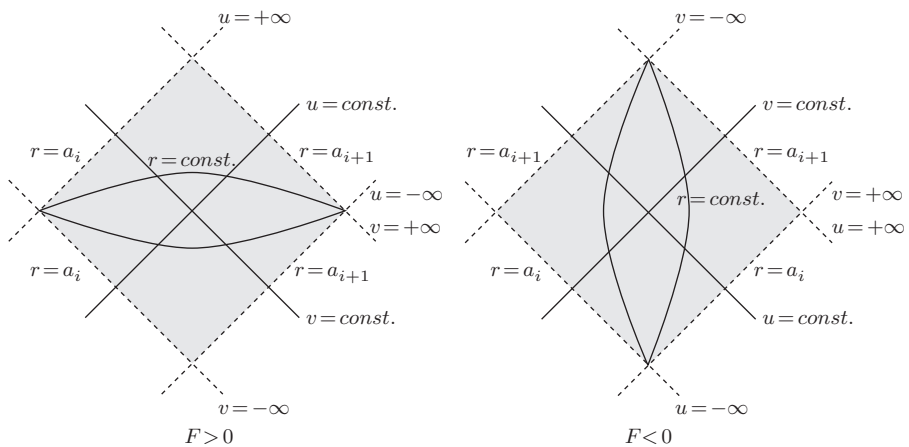


Figure 6.9 Coordinates in a regular block without asymptotic regions; see main text for details.

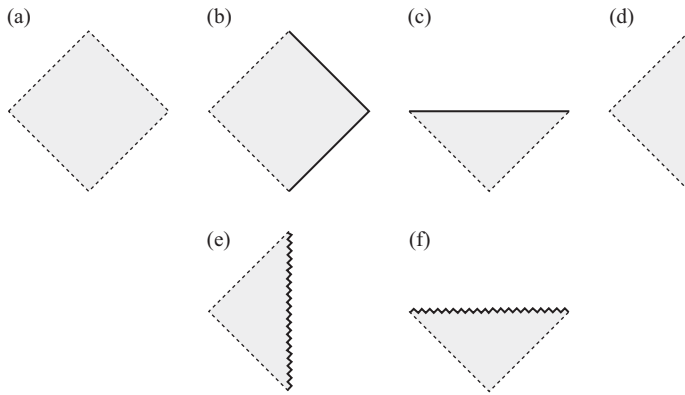


Figure 6.10 Elementary blocks for the construction of Penrose diagrams: (a) non-singular block without asymptotic regions; (b) non-singular block with a null  $\mathcal{S}$ ; (c) non-singular block with a spacelike  $\mathcal{S}$ ; (d) non-singular block with a timelike  $\mathcal{S}$ ; (e) block with a timelike singularity; (f) block with a spacelike singularity.

In the case of blocks  $\tilde{Q}_i$  with  $r \in [a_i, \pm\infty)$  corresponding to asymptotic regions, the metric (6.40) allows us to read out a conformal factor. The particular form of the conformal factor depends on the particular nature of the asymptotic end:

$$\Xi_i = \begin{cases} \cos U_i \cos V_i & \text{if } F(r) \rightarrow 1 \text{ as } r \rightarrow \infty \\ \frac{\cos U_i \cos V_i}{\sqrt{F(r)}} & \text{if } F(r) \rightarrow \infty \text{ as } r \rightarrow \infty. \end{cases}$$

The resulting construction can be depicted in a conformal diagram.

The discussion of the case  $F < 0$  in  $\tilde{Q}_i$  is analogous. In this case the orbits of the Killing vector  $\partial_t$  are spacelike, and the hypersurfaces of constant  $r$  are timelike. The behaviour of the various coordinates in a regular elementary block is summarised in Figure 6.9, right panel. A depiction of the various elementary blocks is given in Figure 6.10.

**Flipping of blocks.** The convention used in drawing the diagrams in Figure 6.9 is that the coordinate  $r$  increases from left to right (if  $F > 0$ ) and from bottom to top (if  $F < 0$ ). As this is a mere convention, it is possible to flip the blocks about  $r_i$ . This operation effectively interchanges the roles of  $u$  and  $v$ . In addition, as the metric  $\tilde{\gamma}$  is independent of the coordinate  $t$ , one has the discrete symmetry  $t \mapsto -t$  which allows further flipping of blocks with respect to the surfaces of constant  $t$  – vertically if  $F > 0$  and horizontally if  $F < 0$ .

**Gluing blocks.** All geodesics such that  $r = a_i$  for some finite value of the affine parameter are incomplete. These geodesics can be extended by gluing blocks along non-singular seams. The convention followed in gluing the blocks is that the time coordinate in each block,  $t$  if  $F(r) > 0$  and  $r$  if  $F(r) < 0$ , changes

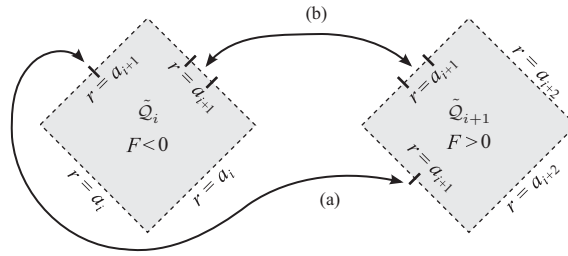


Figure 6.11 The two ways of gluing elementary blocks as discussed in the main text. In the configuration (1) the block  $\tilde{Q}_{i+1}$  has been flipped about  $r_i$ , while in configuration (2) it is necessary to invert its time orientation; see the main text for further details.

vertically. Consider, for example, the gluing of a block  $\tilde{Q}_{i+1}$  with  $F(r) > 0$  and a block  $\tilde{Q}_i$  with  $F(r) < 0$ . By suitably flipping the blocks, they can be glued together in the two ways shown in Figure 6.11. Under the assumption that  $F''$  is smooth at  $r = a_{i+1}$  (and hence also the curvature), the *gluing of blocks* is equivalent to showing that the null hypersurfaces are continuous along the seams, that is, that there is a coordinate system covering both blocks in a neighbourhood of  $r = a_{i+1}$  in a smooth fashion. This construction is implemented through **Eddington-Finkelstein type coordinates**.

As a first example consider configuration (1) of Figure 6.11 where the block  $\tilde{Q}_i$  is glued to a block  $\tilde{Q}_{i+1}$  which has been flipped about  $r_i$ . Direct inspection reveals that while advanced null coordinates exhaust at the gluing seam (i.e. they become infinite), a null retarded coordinate extends to the two blocks  $\tilde{Q}_i$  and  $\tilde{Q}_{i+1}$ . Accordingly, one sets

$$du = dt - F^{-1}(r)dr,$$

so that

$$\tilde{\gamma} = F(r)du \otimes du + (du \otimes dr + dr \otimes du). \tag{6.41}$$

Now, allowing  $r \in [a_i, a_{i+2}]$  one finds that the coordinates  $(u, r)$  cover both blocks in configuration (1) of Figure 6.11 – the resulting combined block is shown in configuration (1) of Figure 6.12. In particular, the coordinate  $u$  is finite at  $r = a_{i+1}$  and the metric (6.41) is smooth for  $r \in (a_i, a_{i+2})$ .

In order to perform the gluing in configuration (2) of Figure 6.11, one needs to flip the block  $\tilde{Q}_{i+1}$  about  $t$ . Direct inspection shows that for this configuration retarded null coordinates exhaust at the gluing seam. Accordingly, one introduces advanced null coordinates

$$dv = dt + F^{-1}(r)dr,$$

so as to obtain

$$\tilde{\gamma} = F(r)dv \otimes dv - (dv \otimes dr + dr \otimes dv). \tag{6.42}$$

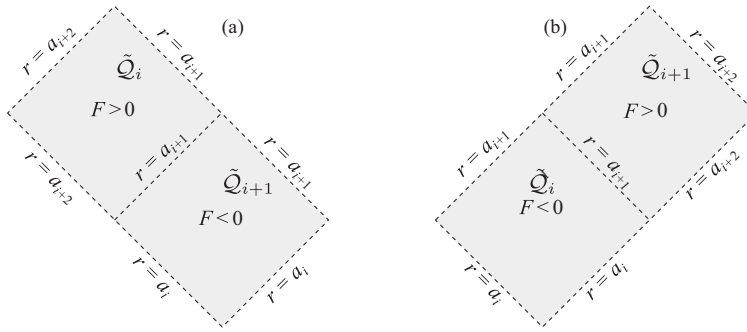


Figure 6.12 The two composite blocks obtained from the the gluing procedures in Figure 6.11.

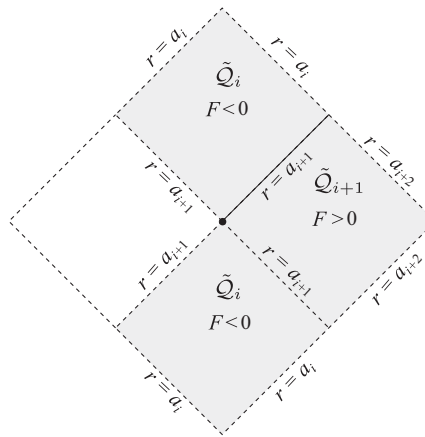


Figure 6.13 Gluing applied to three blocks simultaneously. A fourth block can be glued using the Kruskal construction – see the main text for further details.

The coordinate  $v$  is finite at  $r = a_{i+1}$ . Thus, the pair  $(v, r)$  covers the composite block. One can verify that the metric (6.42) is smooth for  $r \in (a_i, a_{i+2})$ ; the resulting combined block is shown in configuration (2) of Figure 6.12.

**Gluing à la Kruskal.** The gluings discussed in the last paragraphs can be performed simultaneously; the resulting configuration is shown in Figure 6.13. In addition, one could also glue a further region  $\tilde{Q}_{i+1}$  obtained from  $\tilde{Q}_{i+1}$  by applying the reflection in the time coordinate. Notice, however, that the point  $p$  is not covered by either of the coordinates  $(u, r)$  and  $(v, r)$ . Depending on the particular form of  $F(r)$  it may be possible to obtain a single coordinate patch for the four blocks; this is the case, for example, in the Schwarzschild spacetime. The procedure to do this makes use of a generalisation of the **Kruskal coordinates**; see Figure 6.13. The general strategy is to find coordinates  $(U, V)$  such that the metric takes the form

$$\tilde{\gamma} = G(r)(\mathbf{d}U \otimes \mathbf{d}V + \mathbf{d}V \otimes \mathbf{d}U),$$

where  $G$  is bounded and non-zero at  $r = a_{i+1}$ . Since  $U = U(t, r)$  and  $V = V(t, r)$  one readily finds the conditions

$$G\partial_t U\partial_t V = F, \quad \partial_r U\partial_t V + \partial_t U\partial_r V = 0, \quad G\partial_r U\partial_r V = -F^{-1}.$$

It can be verified that a solution to the above is given by

$$U(t, r) = a \exp\left(bt + b \int \frac{dr}{F(r)}\right), \quad V(t, r) = \frac{1}{a} \exp\left(-bt + b \int \frac{dr}{F(r)}\right), \\ G(r) = \frac{F(r)}{b^2} \exp\left(-2b \int \frac{dr}{F(r)}\right),$$

where  $a$  and  $b$  are constants. The function  $G(r)$  given by the above formulae can be singular. The key point in the construction is to analyse whether the constant  $b$  can be chosen so that  $G(r)$  is bounded and non-zero at  $r = a_{i+1}$ . As an illustration, in the case of the *Schwarzschild spacetime* one has that

$$F(r) = 1 - \frac{2m}{r} \quad \text{so that} \quad G(r) = \frac{1}{b^2 r} (r - 2m)^{1-4mb} e^{-2br}.$$

Hence, choosing  $b = 1/4m$  one has

$$G(r) = \frac{16m^2}{r} e^{-r/2m},$$

which is bounded and non-zero at  $r = 2m$ , the location of the horizon. By contrast, in the case of the *extremal Reissner-Nordström spacetime* – see Equation (6.43) – one has

$$F(r) = \left(1 - \frac{m}{r}\right)^2 \quad \text{so that} \quad G(r) = \frac{1}{b^2} (r - m)^{2-4mb} \exp\left(-2br + \frac{6m^2 b}{r - m}\right).$$

In this case one cannot find a value of  $b$  which makes  $G(r)$  finite and non-zero at  $r = m$ . In particular, the choice  $b = 1/2m$  yields

$$G(r) = \frac{1}{4m^2} \exp\left(-\frac{r}{m} + \frac{3m}{r - m}\right),$$

which is singular at  $r = m$ . More generally, if  $F(r)$  is a rational function, it can be shown that the value  $b$  can be chosen so that  $G(r)$  is finite and non-zero at  $r = a_{i+1}$  if  $a_{i+1}$  is a non-repeated zero of  $F(r)$ ; see Walker (1970) for the details of the proof.

Some examples

The procedure described in the previous paragraphs can be employed to construct the Penrose diagrams and conformal compactifications of a number of well-known spherically symmetric spacetimes. In particular, one has the following (details can be found in the given references):

**The non-extremal Reissner-Nordström spacetime.** This is the solution to the Einstein-Maxwell field equations given by the metric

$$\tilde{g} = \left(1 - \frac{2m}{r} + \frac{q^2}{r^2}\right) dt \otimes dt - \left(1 - \frac{2m}{r} + \frac{q^2}{r^2}\right)^{-1} dr \otimes dr - r^2 \sigma,$$

with  $q^2 < m^2$ . In this case  $F(r) = 1 - 2m/r + q^2/r^2$  has two zeros. One can identify three elementary blocks: an asymptotically flat region, a standard regular block and a block with a timelike singularity. In this case Kruskal's construction can be employed to glue four blocks simultaneously. The resulting Penrose diagram is given in Figure 6.14; see Carter (1973).

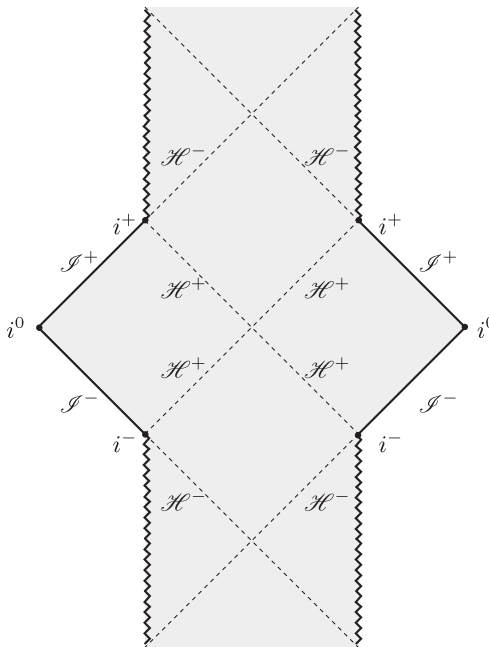


Figure 6.14 Penrose diagram of the Reissner-Nordström spacetime in the non-extremal ( $q^2 < m^2$ ) case. The points  $i^0$  correspond to the various spatial infinities, the points  $i^\pm$  to future and past timelike infinity, respectively, and the lines  $\mathcal{S}^\pm$  to the various components of null infinity. The dashed lines  $\mathcal{H}^\pm$  correspond to the various horizons. Finally, the serrated lines denote the singularities.

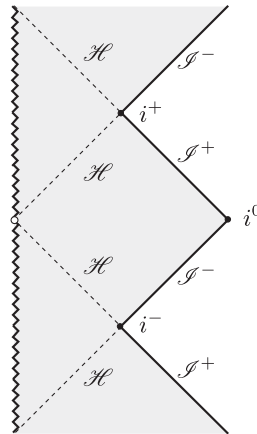


Figure 6.15 Penrose diagram of the Reissner-Nordström spacetime in the extremal case ( $q^2 = m^2$ ). The point  $i^0$  corresponds to spatial infinity, the points  $i^\pm$  to future and past timelike infinity, respectively, and the lines  $\mathcal{S}^\pm$  to the various components of null infinity. The dashed lines labeled by  $\mathcal{H}$  correspond to the various horizons. Finally, the serrated lines denote the singularities.

**The extremal Reissner-Nordström spacetime.** This is the particular case of the Reissner-Nordström spacetime for which  $q^2 = m^2$ . The metric is given by

$$\tilde{g} = \left(1 - \frac{m}{r}\right)^2 dt \otimes dt - \left(1 - \frac{m}{r}\right)^{-2} dr \otimes dr - r^2 \sigma. \tag{6.43}$$

In this case, one has a double zero of  $F(r) = (1 - m/r)^2$ . Thus, one cannot make use of Kruskal’s construction. One can identify two elementary blocks: an asymptotically flat one and a block with a timelike singularity. The resulting Penrose diagram is given in Figure 6.15; see Carter (1966a, 1971). An interesting property of the extremal Reissner-Nordström spacetime is that it is conformally invariant under a certain spatial inversion; see Couch and Torrence (1984). This discrete conformal symmetry can be used to relate properties of null infinity with properties of the horizon; see Bizon and Friedrich (2012). A similar symmetry exists for a particular combination of the parameters in the Reissner-Nordström-de Sitter spacetime; see Brännlund (2004).

**The Schwarzschild-de Sitter and Schwarzschild-anti de Sitter spacetimes.** The metric for these spacetimes is given by

$$\tilde{g} = \left(1 - \frac{2m}{r} + \frac{1}{3}\lambda r^2\right) dt \otimes dt - \left(1 - \frac{2m}{r} + \frac{1}{3}\lambda r^2\right)^{-1} dr \otimes dr - r^2 \sigma,$$

where it is assumed that  $m > 0$ . If  $\lambda > 0$  (the *anti-de Sitter* case), then it can be verified that  $F(r) = 1 - 2m/r - \lambda r^2/3$  has only one real root corresponding to a *black hole-type horizon*. The resulting diagram is given in Figure 6.16. If  $\lambda < 0$  (the *de Sitter* case) and  $0 < -9\lambda m^2 < 1$ , then  $F(r)$  can be shown to have two

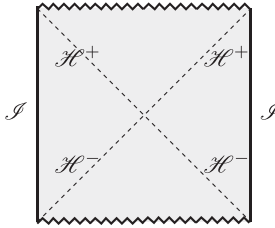


Figure 6.16 Penrose diagram of the Schwarzschild-anti de Sitter spacetime. The vertical lines  $\mathcal{I}$  denote the two components of conformal infinity, while the dashed lines labeled by  $\mathcal{H}^\pm$  denote the various components of the horizon. The serrated lines denote the singularities.

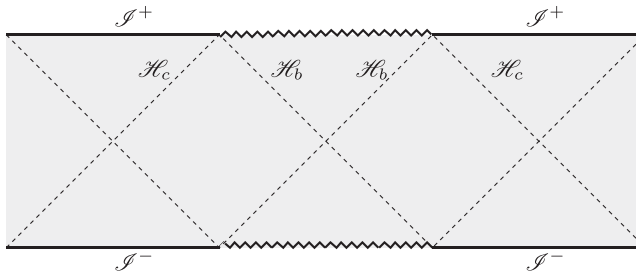


Figure 6.17 Penrose diagram of the Schwarzschild-de Sitter spacetime. The horizontal lines labeled by  $\mathcal{I}^\pm$  correspond to the various components of conformal infinity. The dashed lines  $\mathcal{H}_c$  and  $\mathcal{H}_b$  denote, respectively, the cosmological and black hole horizons. The serrated lines indicate the location of the singularities.

positive real roots corresponding, respectively, to a *black hole-type horizon* and a *cosmological type horizon*. The resulting blocks can be arranged in a periodic diagram as given in Figure 6.17; see, for example, Griffiths and Podolský (2009). In this case it is also possible to make topological identifications; see Beig and Heinzle (2005). The cases  $-9\lambda m^2 = 1$  and  $-9\lambda m^2 > 1$  correspond, respectively, to the so-called *extremal* and *hyperextremal* cases.

Other examples of spacetimes amenable to the general construction described in this section are the Nariai solution, the Reissner-Nordström-de Sitter and the Reissner-Nordström-anti de Sitter solutions; see, for example, Brill and Hayward (1994) for a detailed discussion.

### 6.5.3 Extending across the conformal boundary

In Schmidt and Walker (1983) it has been observed that the conformal representations of some spacetimes can be extended across the conformal boundary. In the case of the Schwarzschild solution this is best seen by considering the metric written in terms of a *retarded null coordinate*:

$$\tilde{g}_{\mathcal{I}} = \left(1 - \frac{2m}{r}\right) \mathbf{d}u \otimes \mathbf{d}u + (\mathbf{d}u \otimes \mathbf{d}r + \mathbf{d}r \otimes \mathbf{d}u) - r^2 \boldsymbol{\sigma}, \quad (6.44)$$

where, in particular,  $u \in \mathbb{R}$ . Defining  $\varrho \equiv 1/r$ , a calculation yields that

$$\varrho^2 \tilde{g}_{\mathcal{S}} = \varrho^2 (1 - 2m\varrho) \mathbf{d}u \otimes \mathbf{d}u - (\mathbf{d}u \otimes \mathbf{d}\varrho + \mathbf{d}\varrho \otimes \mathbf{d}u) - \sigma. \tag{6.45}$$

In this representation, future null infinity  $\mathcal{S}^+$  is given by the condition  $\varrho = 0$ . The key observation is that the metric (6.45) can be analytically extended by allowing  $\varrho$  to take negative values. To identify the spacetime on the other side of  $\mathcal{S}^+$  one undoes the conformal rescaling to obtain

$$\bar{g}_{\mathcal{S}} = (1 - 2m\varrho) \mathbf{d}u \otimes \mathbf{d}u - \frac{1}{\varrho^2} (\mathbf{d}u \otimes \mathbf{d}\varrho + \mathbf{d}\varrho \otimes \mathbf{d}u) - \frac{1}{\varrho^2} \sigma,$$

where  $\varrho \in (-\infty, 0)$ . To bring the metric to a more familiar form one introduces new coordinates  $\bar{r} = -1/\varrho$ ,  $\bar{v} = u$  and defines  $\bar{m} = -m$ , so that

$$\bar{g}_{\mathcal{S}} = \left(1 - \frac{2\bar{m}}{\bar{r}}\right) \mathbf{d}\bar{v} \otimes \mathbf{d}\bar{v} - (\mathbf{d}\bar{v} \otimes \mathbf{d}\bar{r} + \mathbf{d}\bar{r} \otimes \mathbf{d}\bar{v}) - \bar{r}^2 \sigma, \tag{6.46}$$

with  $\bar{r} \in (0, \infty)$  and  $\bar{v} \in \mathbb{R}$ . The metric (6.46) corresponds to the **negative mass Schwarzschild spacetime** in advanced null coordinates. The null hypersurface  $\mathcal{S}^+$  of the conformal extension of the original (positive mass) Schwarzschild spacetime corresponds to the null hypersurface  $\mathcal{S}^-$  of the negative mass Schwarzschild spacetime. It is important to point out that the spacetimes described by the metrics (6.44) and (6.46) are causally disconnected; however, at the level of the conformal structure, they are an extension of each other. This situation is depicted, at the level of Penrose diagrams, in Figure 6.18.

The ideas described in the previous paragraphs can be used to construct so-called **maximal conformal extensions of the Schwarzschild spacetime**. Further details can be found in Schmidt and Walker (1983). The construction described in this section can be adapted to other spacetimes, for example, the Reissner-Nordström solution.

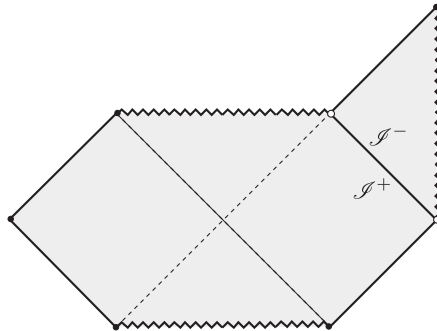


Figure 6.18 Extending the conformal structure of the Schwarzschild spacetime through null infinity. The future null infinity of the positive mass Schwarzschild spacetime is identified with the past null infinity of the negative mass Schwarzschild spacetime, see main text for further details. The points denoted by white dots are excluded from the discussion.

## 6.6 Further reading

The discussion presented in this chapter has been restricted to the analysis of the conformal structure of static, spherically symmetric spacetimes. Some aspects of this discussion can be adapted to the analysis of other exact solutions like the Kerr and Kerr-Newman spacetimes; this is discussed in, for example, Carter (1973), Hawking and Ellis (1973) and Griffiths and Podolský (2009). Another class of spacetimes amenable to an explicit discussion of its conformal structure is that of the Friedman-Lemaître-Robertson-Walker (FLRW) cosmological models; see again Hawking and Ellis (1973) and Griffiths and Podolský (2009).

An alternative discussion of Penrose diagrams of spherically symmetric spacetimes which allows for dynamic configurations can be found in appendix C of Dafermos and Rodnianski (2005). The idea of a Penrose diagram can be adapted to the analysis of suitable two-dimensional timelike totally geodesic hypersurfaces of non-spherically symmetric spacetimes. This idea has been particularly fruitful in the case of the Kerr and Kerr-Newman spacetime; see, for example, Carter (1966b, 1968, 1973), Hawking and Ellis (1973) and Griffiths and Podolský (2009). This strategy, has been adapted to a variety of situations in Chruściel et al. (2012a).